A Review of Natural Circulation Loops in Pressurized Water Reactors and Other Systems

NP-1676-SR

Special Report, January 1981

Prepared by

YORAM ZVIRIN*
Nuclear Power Division
Electric Power Research Institute

*Faculty of Mechanical Engineering, Technion, I.I.T., Haifa, Israel

Electric Power Research Institute
3412 Hillview Avenue
Palo Alto, California 94304

Water Reactor System Technology Program
Nuclear Power Division

ORDERING INFORMATION

Requests for copies of this report should be directed to Research Reports Center (RRC), Box 50490, Palo Alto, CA 94303, (415) 965-4081. There is no charge for reports requested by EPRI member utilities and affiliates, contributing nonmembers, U.S. utility associations, U.S. government agencies (federal, state, and local), media, and foreign organizations with which EPRI has an information exchange agreement. On request, RRC will send a catalog of EPRI reports.

NOTICE

EPRI PERSPECTIVE

PROJECT DESCRIPTION

Natural circulation is a preferred and passive heat transfer mechanism for cooling PWRs. This is valuable for both operational transients and long-term and post-accident heat removal. The experimental and plant data represents an industry resource of great value and potential.

PROJECT OBJECTIVES

It was the intent of EPRI Special Report NP-1676-SR to collate and critically review all available data including those from recently performed reactor tests. All readily available technologies were used in the data base, with particular cooperation from U.S. nuclear utilities.

PROJECT RESULTS

The analysis methods for both turbulent and laminar flow have been reviewed, simple analytic expressions for the loop behavior are given, and the fundamental potential modes of loop instability are identified and given. The available reactor data are collated and compared to the analytic and numerical results. The need for further work in the areas of stability analysis and multidimensional effects is discussed. The report forms a central reference work for natural circulation information and is, therefore, of general use.

Y. Zvirin, Project Manager
Nuclear Power Division

FOREWORD

It has been realized recently that natural circulation cooling of nuclear reactors may have crucial importance under certain conditions, as was the case in the Three Mile Island accident. This review summarizes the available theoretical and experimental methods to investigate steady-state and transient natural circulation flows. Such flows can also become unstable, leading to flow reversals which may impede the heat removal process. The review describes the types of instabilities, and the available methods to treat them.

A section is devoted to nuclear reactor plant data from various tests and actual operational transients. Typical behaviors are illustrated and a comparison is made between the theoretical calculations and the data.

ABSTRACT

A survey is presented on the theoretical and experimental work on single-phase natural circulation loops (thermosyphons). It includes available modeling methods (analytical and numerical) to describe steady state flows, transients and stability characteristics of the various loops. These range from simple geometry systems through small-scale (laboratory) loops to full-scale systems--nuclear reactor plants and solar water heaters.

An attempt is made to compare some of the analytical models and to present the results by using generalized parameters. The available data is given and the comparison with the theoretical results is discussed.

ACKNOWLEDGMENT

The author wishes to thank Dr. R. B. Duffey from EPRI, for his helpful suggestions and comments. Thanks are also due to U.S. utility persons, who helped in acquiring the nuclear reactor plant data: Dr. D. I. Herborn - Portland G.E., E. G. Beasley, J. R. Calhoun, T. D. Knight and J. A. Coffey - TVA, G. R. Bond and N. G. Trikouros - GPU, J. Turnage and A. Husain - Yankee Atomic, R. A. Newton - Wisconsin Electric Power Co., C. R. Steinhardt and M. Marchy - Kewaunee Nuclear Power Plant, R. Hankel and A. Irani - Florida Power & Light Co., R. F. Wardell - Duke Power Co., R. T. Harris - Northeast Utilities Service Co., and M. L. Bowling and G. A. Kann - Virgina Electric and Power Co.

CONTENTS

ILLUSTRATIONS

SUMMARY

In this review, theoretical and experimental results of natural circulation loop (thermosyphons) are surveyed. The loops vary from simple geometry loops, some of which have been treated only theoretically and some in laboratory tests, through small-scale loops relevant to larger systems, and finally full-scale systems for solar water heaters and particularly nuclear reactor plants.

Analytical and numerical modeling methods are presented and discussed. These have been used to obtain the steady-state and transient behavior of thermosyphons and to investigate their stability characteristics. A comparison is provided between the theoretical and experimental results, including the plant data.

Section 1

INTRODUCTION

Natural circulation is created by heating a fluid from below and cooling it from above. The early studies on such flow patterns, starting with Rayleigh's analysis (1), were concerned with the stability of a fluid at rest and the onset of motion due to a temperature gradient in the direction of the body force. A review of external flows caused by buoyancy forces was presented in Ref. (2). Another type of free convection flows is encountered in enclosures and cavities; reviews of the state of the art related to these flows have been given (3-5).

The present review deals with natural circulation loops (thermosyphons), in which heat is convected from a heat source to a higher elevation heat sink. These loops have various applications in energy conversion systems such as solar heaters (6-15) and cooling systems of light water nuclear reactors (LWR) (16-21) and liquid metal fast breeder nuclear reactors (LMFBRs) (22-24). Other applications include geothermal and geophysical processes (25-30). Some of the natural circulation loops in several industrial applications involve two phase flows, e.g., thermosyphon reboilers and absorption cooling systems (31-34), and interest in natural circulation reflux boiling in LWR loops has recently increased (35).

This survey covers mostly single-phase natural circulation loops. It includes a review of available theoretical methods for describing the flow and heat transfer processes, of available experimental results and full scale data of solar systems and nuclear power plants. Figure 1 includes schematics of some of the loops.

It has been observed in experiments, and substantiated by theory, that natural circulation loops can exhibit oscillatory modes of flow, which lead, under certain conditions, to instabilities and to flow reversals (8,10,17,18,26,33). These phenomena have also been investigated in free convection loops of simple geometry (27-30, 36-47). Another mode of instability can also exist in natural circulation loops, namely multiple steady state solutions (under identical conditions) (43-46). A third mode of instability is associated with the onset of motion in the loop, as mentioned above. This mode may also appear as a sudden flow in a previously stagnant branch (18).

The existing theoretical modeling methods for natural circulation loops are reviewed in Section 2. Both analytical and numerical approaches have been used to solve the coupled momentum and energy equations. The results for steady states, transient behavior and stability characteristics are presented.

The effects of the various parameters (geometry, fluid properties boundary and initial conditions, throughflows imposed on loops, etc.) are discussed.

Section 3 includes a survey of the available experimental results, from basic simple geometry loops, small-scale simulation systems and full-scale solar heaters and nuclear power plants. An attempt is made to compare the data on the basis of dimensionless parameters and also to compare the data against theoretical calculations.

Conclusions are given (Section 4) on the performance of energy conversion systems with natural circulation flows, their stability and the accuracy of the theoretical modeling methods compared to the data.

Section 2

THEORETICAL MODELING METHODS

2.1 Basic Assumptions and Governing Equations

The existing theoretical models representing natural circulation loops are based on a one-dimensional approach and follow the outline of the classic theory for buoyancy-driven flows (1-5,29,30). Consider, for example, the loop in Figure 1a; the only spatial coordinate, s, runs around the loop.

A basic assumption in these one-dimensional models is that the average cross section temperature, T, is equal to the mixed mean (or bulk) temperature. It has been further assumed (for the single-phase incompressible fluids in the loops under consideration) that the Boussinesq approximation is valid, i.e., the density, ρ, is regarded as constant (having a reference value ρ_o) in the governing equations except for the buoyancy force term. The latter, of course, is driving the flow by the density variations around the loop . (In some numerical models, changes of the density and other properties with temperature have also been taken into account, c.f. (6,7,47). The fluids, however, are considered incompressible because of the negligible pressure changes in the free convection loops.) Under these conditions, the continuity equation yields the result that the mean velocity, u(t) and the flow rate Q(t) are uniform around the loop and depend only on the time, t. When the flow system includes parallel channels, the flow rates will be uniform in each channel and their sum will be equal to the total flow rate.

Consider now conservation of momentum and energy in the flow. The momentum equation is written in the following manner, for a flow in the positive s direction:

$$\rho_o \frac{\partial u}{\partial t} = \frac{\partial p}{\partial s} - \rho g \hat{e}_z \cdot \hat{e}_s - 4 \frac{\tau_w}{d_H} \qquad (2\text{-}1)$$

where p is the pressure, g is the acceleration of gravity, $\hat{e}_z$ and $\hat{e}_s$ are unit vectors in the vertical (z) and in the s directions and d_H is the hydraulic diameter of the flow channel. τ_w is the shear stress at the wall, which is expressed by $\tau_w = \frac{1}{2} f\rho_o u^2$, where f is the friction coefficient:

$$f = a/Re^b \qquad (2\text{-}2)$$

a and b depend on the flow regime and Re is the Reynolds number, defined by $\rho_o u d_H/\mu$. In most of the theoretical models for thermosyphons the friction factor correlations (or the values of a and b) have been taken as those for fully developed forced flow, e.g., a=16, b=1 for laminar flow and f from the Moody diagram for turbulent flow. However, it has been pointed out by (36,18b,27), these forced flow correlations are not generally valid in natural circulation flows. Since the driving flow mechanism is different in the free convection loops, the velocity distributions are also different; moreover, the flows are frequently not fully developed and in many cases three dimensional flow effects occur. Visual observations (18,37,48) confirm, indeed, these arguments. Thus, for example, comparison of data for temperature differences with analytical results based on forced flow calculations (8,18) shows an uncertainty of order 30%.

Figure 2 includes data for the friction coefficent f in a toroidal loop (36) and an open "square" loop (27), see also Figure 1. It can be seen that the friction factors are higher than those for forced flow. An additional result is the transition zone from laminar to turbulent flow - near Re = 1500, see Figure 2. This transition was also visually observed in the experiments reported on by ref. (36). It is noted, however, that the friction coefficents in Figure 2 cannot be applied to any other free convection loop; the correlations depend, among other parameters, on the loop geometry. It can be expected that they will approach the forced flow correlations in long components, for strong turbulent flows. As mentioned above, the forced flow correlations are used in most cases, due to the lack of more accurate data.

The energy equation is written in the following form:

$$\rho_o c \left(\frac{\partial T}{\partial t} + u \frac{\partial T}{\partial s}\right) - k \frac{\partial^2 T}{\partial s^2} = 4 \frac{q}{d_H} - 4 \frac{h}{d_H} (T - T_o) + \frac{1}{A} \int \Phi dA \qquad (2\text{-}3)$$

where c and k are the specific heat and the thermal conductivity of the fluid, q denotes heat flux input, h is a heat transfer coefficient, T_o is a reference ambient (or wall) temperature and Φ is the dissipation function. The effects of the latter have been neglected in most of the theoretical models. Analysis shows, indeed, that these effects are usually very small, c.f. (40). Only in some extreme cases, such as cryogenic applications, dissipation is significant and would tend to increase the flow rate in a loop (44). Axial conduction (the last term on the left hand side of Eq. 2-3) would tend to decrease the flow in a toroidal loop. These effects are very small and negligible for liquids and gases, and become important only for liquid metals, with small Prandtl numbers Pr.

The heat transfer coefficient, h, has been taken again, from forced flow correlations. Data on the heat transfer parameter is still not available. Heat transfer correlations for laminar and turbulent flows in a toroidal loop have developed by (36); however, since they did not directly measure the flow rate in the loop but derived it from the temperature measurements, their flow resistance and heat transfer data are redundant and can only serve for analogy purposes.

Finally, an equation of state must be added to the momentum and energy Eqs. 2-1 and 2-3. Mathematically, the continuity equation must also be counted to form a set of four equations for the unknown u, T, ρ and p. A detailed solution of the set of coupled equations can be performed only numerically (47). As mentioned above, the interest here is in incompressible flows, where the continuity equation leads to the result that the flow rate is uniform around the loop. The pressure terms can now be eliminated from the momentum Eq. 2-1 by integration around the loop. (Note that the velocity can vary in various components of the loop because of area changes, but the flow rate is constant.)

$$\rho_o \gamma \frac{dQ}{dt} = -g \oint \rho dz - 2\rho_o \oint f u^2 \frac{ds}{d_H} \qquad (2\text{-}4)$$

where the geometrical parameter γ is defined by:

$$\gamma \equiv \oint \frac{ds}{A(s)} \qquad (2\text{-}5)$$

Thus for a loop of a uniform cross sectional area (such as in Figures 1a and 1b, $\gamma = L_t/A$ where L_t is the total circulation length. For most applications the area is uniform in any loop components, and then the integral in Eq. 2-5 can be replaced by the sum.

Eq. 2-4 can be rewritten in the form:

$$\rho_0 \gamma \frac{dQ}{dt} = - g \oint \rho \, dz - \frac{1}{2} \rho_0 R \, Q^2 \qquad (2\text{-}6)$$

where the overall flow resistance parameter R is defined by:

$$R = 4 \oint \frac{f ds}{d_H A^2} \qquad (2\text{-}7)$$

and the integral includes both the frictional losses in the flow channels and the form losses due to bends, valves, etc. (c.f. Eq. 2-2).

Eqs. 2-3 and 2-4 (or 2-6) constitute a set of two coupled equations for u (or Q) and T, where a relation for $\rho(T)$ is also used. In most of the analytical solutions ρ is assumed to depend linearly on the temperature, through a constant thermal expansion coeffocient β:

$$\rho = \rho_0 \left[1 - \beta \, (T - T_0)\right] \qquad (2\text{-}8)$$

In some of the numerical simulations more accurate functions have been used, or a temperature dependence of β.

In order to solve the simultaneous partial differential Eqs. 2-3 and 2-4, boundary and initial conditions must be specified. For the completely closed loop the former are replaced by the requirement that the temperature be continuous around the loop. For an open loop such as in Figure 1d (26-28), an inlet temperature must be given. In other cases, such as a throughflow super-imposed by injection (and extraction) of fluid into the loop (41-45) the mixing processes between impinging streams must be considered. This situation is also encountered when the system includes parallel flow channels. In refs. (41-45) it was assumed that complete mixing is achieved over a very short length. In cases where axial conduction cannot be neglected, conditions of smooth temperature profiles (continuity of the derivatives) must be added.

Finally, stability analyses of the governing equations have been performed to obtain stability characteristics for natural circulation loops, c.f. Section 2.5 below.

Several initial conditions for transient flows have been investigated. The main interest is in two types: (a) uniform temperature and no flow prior to activation

of the heat source (and sink), and (b) initiation of natural circulation from forced flow (e.g., by tripping a pump). The latter may occur in cooling systems such as nuclear reactor loops.

The former type of initial condition (a) would lead to an instantaneous flow in a loop which is not completely symmetric. For symmetric loops, such as in Figures 1a-1d, the bottom part of the fluid may be heated for some time without flow initiation. Welander (30) pointed out that this situation is unstable and therefore any small disturbance will cause a flow in the loop. His argument, however, is based on one-dimensional considerations. Experimental results (27) show that the flow starts only after a significant period of buoyancy buildup. This can be explained by three-dimensional effects leading initially to rather small free convection cells. Only when a critical condition is reached, the buoyancy is strong enough to drive the flow around the whole loop. An expression for a critical Rayleigh number in a symmetrical open loop was derived by (26). There is no information available (neither empirical nor theoretical) on such critical conditions in closed loops.

2.2 Dimensionless Parameters and Scaling

There does not exist, yet, a generally accepted method fo choosing characteristic scaling parameters and non-dimensional groups for natural circulation flows. The available theoretical and experimental results for thermosyphons have been presented in dimensional forms or by dimensionless parameters relevant to the particular case (6-15,18-21,26-30,36-47). It is, therefore, quite difficult to compare results from various loops and to extend the experimental data from small scale systems in order to predict the behavior of large scale (industrial) loops.

The main reason for this problem is the absence of a characteristic velocity - which would be a derived quantity and not a-priori given (as in forced flow). Therefore, the Reynolds number is not a "true" dimensionless parameter representing the flow regimes in the loops and correlations such as shown in Fig. 2 are not "purely" universal.

It has been found (9) that the characteristic velocity $(\beta g L \Delta T)^{1/2}$, used in classical free convection flows near vertical plates or near cylinders, does not represent the steady flow in a natural circulation loop. For the toroidal loop (Fig. 2b), an attempt has been made to define the characteristic velocity by the result of an approximate solution of the steady state (dimensional)

equations, (39,40,45). In these works, the friction coefficients have been correlated by the Reynolds number based on this velocity.

In the following, theoretical and experimental results of free convection loops (steady state, transient and stability) are presented and discussed, mainly on the basis of the original parameters. An attempt is made to correlate some of the results by more general parameters; common trends of loops behavior stemming from similar effects are outlined.

2.3 Steady State Flows

The steady state motion in a natural circulation loop is governed by Eqs. 2-6 and 2-3 without the inertia terms. These are rewritten now, with the assumptions of negligible axial conduction and viscous dissipation and using the relation 2-8, for the density:

$$\frac{1}{2}\rho_o R\, Q^2 = \beta\, g\, \rho_o \oint T\, dz \qquad (2\text{-}9)$$

$$\rho_o\, c\ \ u\frac{dT}{ds} = 4\frac{q}{d_H} - 4\frac{h}{d_H}(T - T_o) \qquad (2\text{-}10)$$

When Eq. 2-10 is written separately for the various components of the loop, then, for example, h=0 in the heat source, q=0 in the heat sink and h=0, q=0 in the connecting pipes. In order to simplify the approach even further, the energy Eq. 2-10 can be solved approximately to yield linear temperature distributions in the heat source and sink. It is noted that this profile is the exact solution for the case of a uniform heat flux input in an insulated heat source. Performing now the integral in Eq. 2-9, the following expression is derived for the flow rate in the loop:

$$Q = \left(\frac{2\,\beta\, g\, \Delta z\, P}{\rho_o c R}\right)^{1/3} \qquad (2\text{-}11)$$

Where P is the total input power and Δz is the equivalent driving head, which is equal to the difference in elevations between the centers of the heated and cooled sections of the loop. Introducing the relation 2-11 for the flow rate into the energy equation, the temperature difference across the heat source is obtained:

$$\Delta T_R = \frac{P}{\rho_o\, c\, Q} = \left(\frac{P}{\rho_o\, c}\right)^{2/3}\left(\frac{R}{2\, g\, \beta\, \Delta z}\right)^{1/3} \qquad (2\text{-}12)$$

The "classic" expressions for Q and ΔT_R represent first approximations and can serve as rough estimates for the steady state behavior of thermosyphons, c.f. (18,21). they have been developed by (21), based on a more simplified approach, for estimates on the flow rates and temperature differences in nuclear reactors. Comparisons with theoretical results, derived by more exact solutions of the energy equation for the solar water heater (9) and the toroidal loop (40), have shown that the deviations are small. These comparisons are further discussed below.

One important conclusion that can be drawn from the expressions 2-11 and 2-12 is that the steady-state values for Q and ΔT_R are independent (to a first approximation, again) of the details of the heat transfer in the heat sink. It is noted, however, that the actual fluid temperature in the loop depends on the heat transfer coefficient.

Another purpose of deriving the relationships 2-11 and 2-12 here is an attempt to define a characteristic velocity and dimensionless parameters for closed thermosyphons. For this we rewrite the overall friction factor R as:

$$R = 4 \frac{L_t}{d_c A_c^2} f_c \qquad (2\text{-}13)$$

where L_t is the total circulation length, d_c and A_c denote now characteristic hydraulic diameter and cross sectional areas in the loop and the friction coefficient f_c is actually defined by the last equation, together with 2-7 and is given by a/Re^b, c.f. Eq. 2-2, where $Re = \rho_o U d_c/\mu$ and U is the characteristic velocity, $U = Q/A_c$. Introducing these relations into 2-11 we obtain:

$$U = \left(\frac{\beta\, g\, \rho_o^{b-1} d_c^{b+1} \Delta z\, P}{2\, a\, c\, \mu^b\, L_t A_c}\right)^{1/(3-b)} \qquad (2\text{-}14)$$

The last expression reduces to the one obtained in (36,40) for the toroidal loop, where $\Delta z = 4r_2/\pi$ is the elevation difference between the centers of gravity of the heated and cooled sections and the total power is given by $P = 2\pi^2 r_1 r_2 q$. For laminar flow where a=16 and b=1, Eq. 2-14 yields:

$$U = \left(\frac{\beta\, g\, d_c^2\, \Delta z\, P}{32\, c\, \mu\, L_t A_c}\right)^{1/2} = \left(\frac{\beta\, g\, \Delta z\, P}{8\, \pi\, c\, \mu\, L_t}\right)^{1/2} \qquad (2\text{-}15)$$

It is noted that Eq. 2-15 is valid only in cases where the shear stress in the loop is dominated by friction losses in the channels and not by form losses (which are proportional to U^2). As mentioned above and can now be seen from Eq. 2-15, the characteristic velocity is not of the form $(\beta g L \Delta T)^{1/2}$.

For strong turbulent flows, where it can be assumed that the friction coefficient is constant $f_c = f_w = a$, b=0, eq. 2-14 reduces to:

$$U = \left(\frac{\beta\, g\, d_c\, \Delta z\, P}{2\, f_w\, c\, \rho_o\, L_t A_c}\right)^{1/3} \qquad (2\text{-}16)$$

which is essentially the relation 2-11 with R defined by 2-13.

Finally, the main effects of the various parameters, (including geometry and fluid properties) on the loop flow rate, Q, and temperature difference over the heat source ΔT_R, can be seen from Eqs. 2-11 through 2-16. As could be expected, Q increases (and ΔT_R decreases) with the thermal expansion coefficient, the input power and the elevation difference between the heat sink and source. The specific heat and the viscosity and total circulation length or overall friction have the opposite effects.

The approximate expressions 2-11 - 2-16, derived by assuming linear temperature distributions, will serve as a basis for comparision for various loop results. The theoretical solutions of steady-state motions are governed by Eqs. 2-9 - 2-10. The method of approach for analytical treatments, when all the properties are considered constant, is as follows: the energy Eq. 2-10 is first solved for each component of the loop and the constants of integration are found from the requirement of temperature continuity around the loop. At this stage the flow rate, Q, is taken as an unknown constant. Then the temperature distribution is used to perform the integral in Eq. 2-9, resulting in an algebraic equation for Q. The solution of this equation can be substituted into the expressions for the temperature profiles. It is noted that numerical methods have usually been utilized to solve loop transients, to be discussed later.

In order to compare theoretical and experimental results of various loops, a presentation based on nondimensional parameters should be adopted. For this, Eqs. 2-9, 2-10 can be rewritten in a dimensionless form by scaling the flow rate

by Q_{ch}, given by one of the expressions 2-11, 2-14 through 2-16, the temperature $T - T_0$ by q/h, and the lengths by Δz:

$$Q^2 = G \oint T \, dz \tag{2-17}$$

$$G \, Q \frac{dT}{ds} = \begin{cases} M_1 & \text{heat source} \\ -M_2 T & \text{heat sink} \end{cases} \tag{2-18}$$

where Q, T, Z and s are nondimensional, here, M_1 and M_2 are geometrical factors involving ratios of various lengths, perimeters and cross-sectional areas in the heat source and the heat sink. The parameter G, defined by:

$$G = \frac{2 \beta g \Delta Z q}{R h Q_{ch}^2} \tag{2-19}$$

is related to the Grashof number. As can be seen, the steady state motion in natural circulation loop is dominated by this dimensionless parameter and the loop geometry. It is noted that the form of Eq. 2-17 and the characteristic flow rate in Eq. 2-19 may change, depending on the flow regime and the assumed form of the friction correlations.

It is emphasized that the choice of the characteristic flow rate, temperature and length and that of the dimensionless parameter G (Eqs. 2-11 through 2-19) is rather arbitrary. In most of the existing works reported here, where the results have been presented by dimensionless groups, these are of different form. As an example, Figure 3 includes steady-state results for the flow rate and temperature difference across the heated section in the vertical and toroidal loops, Figs. 1a, 1b. As can be seen, the various definitions of the scaling and dimensionless parameters make it difficult to compare the results. One conclusion, however, can be drawn--the flow rate in the loops increases, and the temperature difference ΔT_R decreases, with the modified Grashof number, as could be expected. Figure 3a also includes the experimental results from the toroidal loop (36); the agreement between the theory and the data here is good. The subject is discussed further in Section 3.

2.4 Transient Behavior

The time-dependent Eqs. 2-3 and 2-4 or 2-6, govern the flow and temperature distributions in natural circulation loops. Unlike the steady-state cases where

the equations can be uncoupled, there is no general approach to treat transient behavior, and the equations must be solved simultaneously.

An integral method has been used to transform the equations for the vertical loop, Fig. 1a, into a set of ordinary differential equations in time, and those were solved numerically (38). Finite difference numerical methods have been applied to derive the transient behavior in the toroidal loop, Fig. 1b, (39,47) and a solar water heater, Fig. 1f, (6,7). Typical results are shown in Figs. 4-6. It is noted that an additional parameter, related to the time constant of the system, appears in the transient equations. There is no general approach for choosing this additional parameter. Therefore it is difficult, again, to compare transient results from different loops. A lumped-parameter method has been used (18) to calculate the transient behavior of the average system temperature in an experimental rig relevant to a PWR loop (Fig. 1e). The main purpose of that calculation was to follow the general trend of the transient, and to estimate the time constant. The results are shown in Fig. 7, which also includes the data from this loop.

For the transient solutions, initial conditions must be specified. Two types are usually of more interest: initiating a flow from rest and establishment of natural circulation from forced flow. The latter is important in nuclear reactor cooling loops when the primary pumps are tripped and the decay heat in the core must be removed by natural circulation.

It has been pointed out (30) that the rest state of a thermosyphon is always unstable (when the heat source is applied). A linearized method (27) was used to investigate the stability of the rest state in the loop shown in Fig. 1d. The results show, indeed, that there is always an unstable mode (or a disturbance will always grow). However, the data from this loop (27), shown in Fig. 8a, shows that the loop flow was initiated only long after activation of the heater. This implies that these predicted instabilities are local in nature and probably cause only closed convection cells (of the Benard type), while another critical condition must be reached prior to initiation of a circulation flow in the loop. This agrees also with the results of (18), shown in Fig. 8b, for flow initiation in one stagnant branch (while the other loop was active) of a system similar to that in Fig. 1e. Recent data obtained in a two-phase natural circulation loop show similar behavior (48). It is noted that while the former instabilities are not enough to initiate a flow from rest in a symmetrical loop (Figs. 1a-d), a circulation will start immediately when the heat source is applied to a nonsymmetrical

loop such as in Fig. 1f. Furthermore, an "artificial" initial condition of some weak flow or some temperature penetration depth must be assumed in order to solve (from rest) the transient equations of a symmetrical loop, c.f. Figs. 4, 5.

For the other initial condition, i.e., natural circulation following forced flow in the loop, the flow rate and temperatures undergo some oscillations (over- and under-shoots) before reaching the steady state, see Fig. 6. Similar results have been obtained by using a numerical code (RETRAN) to calculate the transient of natural circulation establishment in the Three-Mile Island plant (about 30 days after the accident), see Fig. 9 and ref. (20).

2.5 Stability Characteristics of Natural Circulation Loops

As mentioned above, single phase thermosyphons may exhibit unstable flows under certain conditions. The stability of the rest state was discussed above, and in this section stabilities of flows in various loops are reviewed. Two additional types of instabilities have been observed (experimentally) and analyzed (theoretically): small-amplitude oscillations that grow and may lead to flow reversals, and multiple steady state solutions (or meta-stable equilibria). Both analytical and numerical methods have been used to investigate these phenomena and to find stability boundaries (or marginal stability curves).

The analytical approach to the small amplitude instabilities is based on the method suggested by (30). The flow rate and the temperature are written in the following forms:

$$Q(t) = \bar{Q} + \Psi\, e^{\sigma t};\quad T(s,t) = \bar{T}(s) + \phi(s)e^{\sigma t} \qquad (2\text{-}20)$$

where $\bar{Q}$ and $\bar{T}$ denote steady state values, Ψ and ϕ small perturbations and σ is the stability parameter. The perturbations will grow if the real part of σ (which is generally a complex number) is positive. Thus marginal stability curves, which separate between stable and unstable zones in the parametric space chosen to represent the system, are the loci of Real(σ) = 0. It is interesting to note here that in all cases where this type of instability has been found (either experimentally or theoretically), it is of the oscillatory mode (Imag (σ) $\neq$ 0). The reason for it stems from the physics (or mechanism) underlying the growing disturbances: imagine a pocket of fluid entering the heat source at a temperature higher than the "usual" and flow rate smaller than the "usual" (because the oscillations of T and Q are not necessarily in phase). This fluid pocket will emerge

even hotter from the heat source. For certain conditions the time lag until this fluid pocket will enter the heat sink can be such that the temperature then will be higher, again, and the flow rate also higher than "usual", which will increase the perturbation. The process can be continued until a flow reversal occurs or nonlinear effects become significant and cause decay of the perturbations.

In order to calculate the stability parameter σ, Q and T from Eq. 2-20 are introduced into the time-dependent Eqs. 2-3 and 2-4 or 2-6. The steady-state relations are identically eliminated and then the equations are linearized by neglecting second order terms (Ψ^2, ϕ^2 and $\Psi\phi$). The linearized perturbation energy equation is solved for the temperature distribution $\phi(s)$, using also the boundary (or continuity conditions). The integral in the perturbation momentum equation is performed, resulting in an algebraic equation for σ. (Note that this equation is homogeneous in Ψ, which can therefore be dropped. The actual values of Ψ and ϕ, which are determined by initial conditions for the perturbations, are not important for the marginal stability treatment.) The values of σ can be found by solving the equation, or an equivalent method, e.g., the Nyquist criterion (36), can be used to obtain the marginal stability curves.

Figures 10a and b show the stability characteristics of the simple geometry loops (Figs. 1a and 1b). The data obtained (36) on the stability of the toroidal loop is also included in Fig. 10b. In these experiments (36), flow oscillations and reversals were observed both visually and by measuring the temperature difference ΔT_R, see Fig. 10c.

Another method of attaining the stability characteristics of the loops is to employ the numerical solutions of the time-dependent equations, starting from some perturbations to the steady state. The numerical results of Greif et al. (39) and Kaizerman et al. (47) for the toroidal loop (Fig. 1b) fit closely the analytical ones of Creveling et al. (36) and Zvirin (40).

An analytical investigation of the stability of solar water heater was performed (10,49). The results showed that any instabilities that may exist lie well outside the practical range of parameters of the system. Another interesting result from this study (10,49) is that there may be oscillatory modes which decay rather slowly. The data obtained (8) (to be discussed in Section 3) shows, indeed, the existence of such oscillations, see Fig. 12.

The other type of thermosyphon instability, namely, the multiple steady state solutions, has been discovered (experimentally and theoretically) (46) for the parallel-tubes loop (Fig. 1c), see Figure 11a. It has also been found analytically (43,45) that multiple steady-state solutions can be encountered when a throughflow is superimposed on the (otherwise closed) thermosyphon. This happens at relatively high inlet temperatures of the throughflow, see Fig. 11b. It has been shown (43) that there is no relation between the two types of instabilities in the vertical loop (Fig. 1a), and the small-amplitude stability of the multiple solutions depends on the system parameters such that either or both can be stable or unstable. The general effect of the throughflow, however, is to stabilize the flow in the loop, see Fig. 11b. Multiple steady-state solutions have also been found analytically for the toroidal loop (Fig. 1b) with angular displacement of the heat source and sink (37). The experiments reported on in ref. (37) did not include these cases.

As mentioned above, an instability leading to a flow reversal was also observed in a loop similar to that in Fig. 1e, see Fig. 8b and ref. (18). The reference does not include a stability analysis of this phenomenon; it might have been caused by either type of instability, but more probably by the one related to the onset of motion, discussed in Section 2.4, since the flow reversal occurred in a previously stagnant branch of the loop.

Finally, it is noted that natural circulation loops, and particularly with asymmetries such as caused by parallel branches or throughflows, may exhibit instabilities, flow oscillations and also flow reversals. These may hamper the performance of thermosyphonic energy conversion systems, such as solar water heaters and nuclear reactor cooling loops (under conditions such as throughflows or makeup liquid to compensate for leaks or small breaks). The analysis of such instabilities must be carried out carefully; it has been shown (38) that assumptions regarding the temperature distributions in the loop (which may be justified for steady-state and transient calculations) lead to completely wrong stability characteristics.

Section 3

EXPERIMENTAL WORK ON NATURAL CIRCULATION LOOPS

3.1 Small-Scale Experiments

Although there has been considerable amount of data on natural circulation loops in large systems--nuclear reactor plants--see Section 3.2, there have been relatively few experimental studies of small-scale thermosyphons. A summary of the available results is presented here; some of them have alredy been mentioned and discussed in the previous section. The simple-geometry loops investigated experimentally include the toroidal one (Fig. 1b) (36,37), the parallel tubes (Fig. 1c) (46) and the open thermosyphon (Fig. 1d) (27,28). Tests have also been performed on a parallel-loop system relevant to a PWR (Fig. 1e) (18) and solar water heaters (Fig. 1f) (6,8). Data from nuclear reactor plants are also available including tests and actual transients. It is noted that any new nuclear power plant must run a natural circulation test as one of the requirements for operating training (16).

In general, all the available data on thermosyphons confirm the trends, behaviors and characteristics of the loops, discussed in Section 2, above. (Naturally, some of the analyses have been carried out in order to explain observed phenomena.)

The data on the toroidal loop (36) are shown in Fig. 3. In this case, the theoretical calculations closely fit the experimental results. The reader is reminded, however, that the frictional coefficients for laminar and turbulent flows in the loop were determined by the results for the flow rates, (see also Figure 2). In all the other studies on closed-loops natural circulation, where forced-flow friction and heat transfer correlations are used, the deviations between theory and data are typically of the order ± 30%. These deviations follow mainly from the assumptions of one-dimensional fully developed flow and the adoption of the above-mentioned forced-flow relationships. The discrepancies between theory and data appear in both steady-state and transient flows. Examples are shown in Figures 6 and 12 for the solar water heater, Figure 8a for the open thermosyphon (Fig. 1d) and the plant data from Three Mile Island--Figure 9. It is noted that in the latter case the flow resistance for the damaged core was not

known, which leads to increased uncertainties. Other plant data are presented and discussed below. Finally, experiments have been performed on a natural circulation system relevant to a PWR, with two parallel loops including once-through heat exchangers (18). The vessel, including the heated section and parts of the connecting pipes (legs), was transparent. The experiments included investigation of the geometrical effects of varying flow resistance in the heated section, arrangement of the heaters and the upper-plenum design. The flows were indeed found to be three-dimensional, and the geometrical variations contributed to such effects as internal recirculation zones and buoyant rising jets (thermal plumes).

As mentioned in Sections 2.4 and 2.5, theoretical investigations of natural circulation loops show three types of possible instabilities: (1) one associated with the onset of motion (either in the whole loop or in a stagnant branch), (2) the growth of flow and temperature oscillations, which may lead to flow reversals, and (3) the multiple steady-state solution (or meta-stable equilibrium). The available results from experimental studies on thermosyphon confirm the existence of these three modes of instabilities.

The first one (onset of motion) was observed in the open loop (Fig. 1d) (27), where the outlet temperature started changing a long time after activation of the heat source, see Fig. 8a. The numerical solution of the coupled momentum and energy equation shows the general trend of the transient, including the first strong oscillation of the temperatures and the subsequent weaker oscillations. However, the calculations significantly overpredict the temperature values.

In the loop relevant to a PWR (Fig. 1e) (18), a similar phenomenon was discovered during a one-loop operation. A flow in the reversed direction occurred suddenly in the (previously) inactive, or stagnant, loop. The mechanism for these flow onsets is the buildup of a buoyancy difference of heavier (cooler) fluid on top of lighter (hotter) layers. At some point, a critical condition is reached where this buoyancy force is strong enough to drive a flow around the loop. A similar effect may occur in a two-phase natural circulation loop.

The second type of instability, i.e., oscillation growth, was observed in the toroidal loop (Fig. 1b) (36). Typical behavior of the growing temperature oscillations leading to flow reversals is shown in Fig. 10c. The data points for stable and unstable flows in the stability map, Fig. 10b, confirm the theoretical deviations of the marginal stability curve; the agreement between the theoretical calculations and the data is quite good.

Oscillations in the flow rate and temperatures have also been observed in solar water heaters, c.f. (8). Fig. 12 shows data taken on a clear day, with no significant fluctuations of the impinging solar radiations. The oscillations in the flow rate have a slow decay mode, and a period of about 1500 sec, but no instabilities and no flow reversals were observed. This is in accordanace with the theoretical results (10,49) that the system is stable in the practical range of its parameters, and has a slowly decaying mode of oscillations.

The third type of instability is associated with multiple steady state solutions. Fig. 11a shows theoretical results for a loop consisting of three parallel tubes (Fig. 1c) (46). In the experiments, it was observed that a critical heat input exists in a second channel for a fixed input in the first channel. Above the critical value, the flow in the second channel was always upwards. However, below it the flow in the second channel could be reversed by disturbances such as a temporary restriction of the third channel or a short injection of a falling jet in the second channel. Recent data on a natural circulation system, having parallel loops with U-tube heat exchangers (48), show that bidirectional flows can exist in stagnant branches. By letting a temporary flow of secondary coolant liquid in these loops, it is possible to change the flow pattern such that it becomes unidirectional.

3.2 Nuclear Reactor Plant Data

As mentioned above, the information on natural circulation loops in nuclear reactors derives from plant data on this mode of cooling from either planned tests or from operational transients. The planned tests have been conducted either for the main purpose of observing the plant performance under natural circulation or for simulating a more general incident, e.g., loss-of-offsite power. The operational transient data on natural circulation have been obtained during plant incidents such as actual loss-of-offsite power, reactor scrams after which the coolant pumps had to be tripped because of the excessive loads or, in for more extreme case of postaccident heat removal, as for the Three Mile Island plant.

The data from pressurized water reactors (PWRs), see also refs. (50,51), include mostly hot- and cold-legs temperatures, pressures in the primary coolant and pressures and water levels in the pressurizer and in the secondary sides of the steam generators. In all cases, transient behavior was monitored from the initiation of the test or incident. In some cases, steady or quasi-steady states were reached. Reference (52) discusses some aspects of transition between single- and two-phase

natural circulation flows in plants. Some of the phenomena that occurred during the accident at TMI-2 are described.

A summary of the available plant data is given in Table 1*, specifying the type of test/incident which occurred. The natural circulation tests carried out in nuclear reactors can be generally divided into two types: (a) onset of motion from rest, by increasing the reactor power to a few percent (1%-4%) of the capacity, and (b) transition from forced flow to natural circulation by scramming the reactor (after continuous operation at some significant power) followed by pumps trip. As mentioned above, the purpose of the first type of tests is observing general behavior of the system in natural circulation; in some cases, one objective may be verifying a computer code [e.g., Trojan (No. 17 in Table 1)]. The purposes of the second type of tests is to simulate an actual operational transient, such as a loss-of-offsite power. These tests can either be terminated after less than two hours (by resuming operation of the reactor primary cooling pumps) or can run for several hours to cold shutdown, usually by the Residual Heat Removal (RHR) system.

The plant operational transients with natural circulation, listed in Table 1, include actual loss-of-offsite power (in which the reactor is immediately scrammed), an incident where the reactor was scrammed by an erroneous separation from the grid, shutdown because of various failures such as turbine blade failure, hot reserve auxiliary bus, and steam generator tube leakage. In the latter cases, the pumps were tripped and natural circulation was established and maintained for long periods of time (hours or days), until cold shutdown with the RHR could be achieved. Ref. (50,51) mention some additional operational transients in which natural circulation took place: reactor pump seal failure or other pump failures (at full or low power) and stuck open steam dump valve. However, these references (50,51) do not provide any data for these transients.

During cooldown by natural circulation, the primary liquid volume contracts; this may cause depressurization and void formation in the reactor vessel, which may hamper the natural circulation flow. Therefore, it is essential to keep the primary liquid pressurized or to maintain the inventory at "water-solid" (i.e., completed filled). This can be done by either having the High-Pressure-Injection

*The table includes data provided by U.S. utilities and additional data from Refs. (50,51). These references mention tests and incidents in other plants, but do not provide any data.

System (HIPS) operating or controlling the primary conditions by the pressurizer (heaters or water spray). An example of the latter is illustrated in Fig. 16 and discussed below.

Finally, natural circulation also occurred during the accident at the Three Mile Island (TMI-2) plant, which started from a loss of feedwater to the steam generators, accompanied by a stuck-open relief valve. This flow, however, was two-phase and not effective for the decay heat removal, resulting in the core uncovery, c.f. (52). A month later, single-phase natural circulation was established and maintained for an extended period of time for cooling the damage core.

Table 1 includes the steady- (or quasi-steady) state values of the temperature difference (between the hot and cold legs) and the core mass flow rate, based on a heat balance for the core. The calculated ΔT in the table were obtained by Eq. 2-12, and estimates for the driving head Δz and the overall friction parameter R, as explained in the following section.

3.3 Comparison of Plant Data to Analysis

The driving head in Eq. 2-12 (see also (21)) is taken as the difference in elevations between the center of the core (the heat source) and the steam generator (the heat sink). The flow resistance parameter R is taken as that for forced flow in the system. For this we write (based on the definitions in Sections 2.2 and 2.3 above), assuming turbulent flow (which is always the case in the large systems under consideration):

$$\Delta p_N = \frac{1}{2} \rho_o \, R \, Q_N^2 \qquad (3\text{-}1)$$

where Δp_N is the overall pressure drop in the loop and Q_N is the volumetric flow rate in the core under nominal operating conditions, i.e., plant design data. The value of R from Eq. 3-1 can be used in Eq. 2-12 for ΔT when all the existing primary loops are active and natural convention flows take place in them. In some cases, the number of operating loops in natural circulation can be lower, while the other loops are inactive, e.g., because of problems in the steam generator feedwater. The value of R has to be modified then as follows, c.f. (18). The pressure drop in one complete loop is separated into the core $-\Delta p_c$ and the rest of the loop - Δp_L (see also Fig. 1e):

$$\Delta P_N = \Delta P_c + \Delta P_L = \frac{1}{2} \rho_o \, R_c \, Q_N^2 + \frac{1}{2} \rho_o \, R_L \left(\frac{Q_N}{n}\right)^2 \equiv \frac{1}{2} \rho_o \, R_1 \left(\frac{Q_N}{n}\right)^2 \qquad (3\text{-}2)$$

where R_c and R_L denote the friction parameter for the core and the rest of the one loop (respectively), R_1 is the friction factor defined for a complete circulation in one loop and n is the number of existing loops in the plant. Eq. 3-2 is based on symmetrical flow split in nominal operating conditions. The friction factor R, for one-loop operation is, from (3-2):

$$R_1 = R_L + n^2 R_c \tag{3-3}$$

For natural circulation in ℓ loops, the overall resistance factor can be obtained in a similar way:

$$R_\ell = R_1/\ell^2 \tag{3-4}$$

It follows that the overall "nominal" value of R is related to R_L and R_c by $R = R_c + R_L/n^2$. It is noted that R_L has to include the resistance of the locked-rotor pump. Since a K-factor is used to express this resistance, the additional term would be K/A^2 where A is the cross-sectional area (inlet or discharge), corresponding to K.

The values of Δz and R are introduced into Eq. 2-12 to calculate the temperature difference ΔT between the hot and cold leg. ρ_0 and the other fluid properties are taken at the average temperature.

It is noted that the calculated values can be served as rough approximations only. As mentioned above, the adoption of forced flow correlations and the use of Eq. 2-12, based on a one-dimensional approach, lead to uncertainties of order ±30%. Moreover, the data on the power is not accurate and, in many cases, the accuracy may be close to 1% of full power--which is significant compared to the power levels during incidents and tests. Most of the temperatures, measured by thermocouples, were acquired on strip-chart recorders, which, again, are not very accurate. On the other hand, however, the transients involved in natural circulation, and even the change from forced flow to this mode of cooling, are rather slow--the time constants are usually of the order of at least several minutes.

There are only a few available calculations of transient behavior of nuclear reactor plant in natural circulation flows. As has been shown in Section 2.4, the momentum and energy equations for the loop cannot be uncoupled, and numerical methods must be used in order to solve them. Figure 9 illustrates calculations

for natural circulation behavior of TMI-2 after the accident, by using the RETRAN code. The same code has also been used to simulate the test in the Trojan plant, see No. 17 in Table 1.

The general trends of the transients in the tests or incidents are described in Table 1. Figs. 13-16 include the typical behavior of flow rates, temperatures, pressures and levels in the pressurizer and steam generator of various plant designs. Figure 13 shows a comparison between a simplified analytical approach (using Eq. 2-12) and data from 3- and 4-loop steady operation in tests at Zion-1. The agreement is within the accuracy bounds mentioned previously. Figures 14 and 15 depict typical behavior of the hot- and cold leg temperatures in a transition from forced to natural circulation. Temperature oscillations (undershoots and overshoots) can be seen, similar to those in simple geometry loops, see Section 2.3 and Fig. 5.

Fig. 16 is of particular interest; it shows the depressurization of the primary liquid after establishment of natural circulation following reactor scram because of loss-of-offsite power in two different incidents at St. Lucie (see also Table 1, nos. 25,26). The fast depressurization caused steam generation and a steam bubble formed in the reactor dome. However, the natural circulation flow was not hampered in these cases because the two-phase mixture level was well above the hot legs. The operators dimished the void by repeatedly spraying water into the pressurizer and adding makeup flow, as can be seen from the level behavior in Fig. 16. It is noted that penetration of steam into the hot leg may impede the single-phase natural circulation leading to two-phase circulation. Further depletion of inventory may lead to core uncovery (19,20,35,48).

Section 4

CONCLUSIONS

As demonstrated by the information reviewed, natural circulation can serve as effective means of transferring heat from a heat source to a higher-elevation heat sink in a flow loop (thermosyphon). In most cases, transients lead to steady or quasi-steady flows. The latter, which can also be termed very slow transient, is encountered in the two main applications of natural circulation loops--decay heat removal from nuclear reactor cores and thermosyphonic solar water heaters. The existing theoretical modeling methods yield approximate results (of the order $\pm$30% compared to data) and can reconstruct general system behavior and trends during transients. For example, the theory shows oscillations and over- and undershoots of flow rate and temperatures after transition from forced to natural circulation in loops.

The theoretical results also show the three types of instabilities, observed in experiments with thermosyphons: (a) the onset of motion in the whole loop or in a stagnant branch; (b) small amplitude oscillation growth, which can lead to flow reversals; and (c) multiple steady-state solutions in nonsymmetrical systems such as parallel branches or superimposed throughflows.

The available modeling methods are not always capable of predicting the stability characteristics of general loops, and generalized criteria for the unstable situations are still lacking. Moreover, the results of stability analyses are very sensitive to assumptions made in the modeling of the loop, e.g., linear temperature distributions. However, progress is being made by advanced analytical and numerical methods.

It is quite difficult to compare between various theoretical results, expecially for different loops, and between theory and data. The reason is the lack of scaling laws or a general approach for choosing characteristic quantities and dimensionless parameters. A first attempt in this direction has been made here.

Finally, the existing analytical and numerical methods representing natural circulation loops are one-dimensional. The flows, however, have been observed to give rise to three-dimensional effects. These should be taken into account in future work, by more detailed analysis, using the three-dimensional conservation equations, and by more sophisticated experiments, including measurements of transverse velocity and temperature distributions.

Section 5

REFERENCES

1. Lord Rayleigh. "On Convection Currents in Horizontal Layers of Fluid when the Higher Temperature is on the Underside." Phil. Mag, Vol. 32, 1916, pp. 529-546.

2 B. Gebhart. "Natural Convection Flows and Stability." In Advances in Heat Transfer (J. P. Hartnett and T. F. Irvine, Jr.), Vol. 9, 1973, pp. 273-348.

3. S. Ostrach. "Natural Convection in Enclosures." In Advances in Heat Transfer (J. P. Hartnett and T. F Irvine, Jr.), Academic Press, New York, Vol. 8, 1972, pp. 156-222.

4. I. Catton. "Natural Convection in Enclosures." Proc. of the 6th Int. Heat Transfer Conference, Toronto, Canada, Vol. 6, 1978, pp. 13-31.

5. D. Japikse. "Advances in Thermosyphon Technology." In Advances in Heat Transfer, (T. F. Irvine, Jr. and J. P. Hartnett, eds.), Academic Press, Vol. 9, 1973, pp. 1-111.

6. K. S. Ong. "A Finite Difference Method to Evaluate the Thermal Performance of a Solar Water Heater." Solar Energy, Vol. 16, 1974, pp. 137-147.

7. K. S. Ong. "An Improved Computer Program for the Thermal Performance of a Solar Water Heater." Solar Energy, Vol. 18, 1976, pp. 183-191.

8. A. Shitzer, D. Kalmanoviz, Y. Zvirin and G. Grossman. "Experiments with a Flat-Plate Solar Water Heating System in Thermosyphonic Flow." Solar Energy, Vol. 22, 1979, pp. 27-35.

9. Y. Zvirin, A. Shitzer and G. Grossman. "The Natural Circulation Solar Heater-Models with Linear and Nonlinear Temperature Distributions." Int. J. Heat Mass Transfer, Vol. 20, 1977, pp. 997-999.

10. Y. Zvirin, A. Shitzer and A. Bartal-Bornstein. "On the Stability of the Natural Circulation Solar Heater." Proceedings of the 6th International Heat Transfer Conference, Toronto, Canada, Vol. 2, 1978, pp. 141-145.

11. T. Jasinsky and S. Buckley. "Thermosyphon Analysis of a Thermic Diode Solar Heating System," ASME, 77-WA/Sol-9, 1977.

12. G. L. Morrison and D.B.J. Ranatunga. "Transient Response of Thermosyphon Solar Collectors." Solar Energy, Vol. 24, 1980, pp. 55-61.

13. G. L. Morrison and D.B.J. Ranatunga. "Thermosyphon Circulation in Solar Collectors." Solar Energy 24, 1980, pp. 191-198.

14. A. Mertol, W. Place, T. Webster, and R. Greif. "Thermosiphon Water Heaters with Heat Exchangers." AS/ISES Conference, Phoenix, Arizona, June 2-6, 1980 (Lawrence Berkeley Laboratory Report, LBL-10033, 1980).

15. A. Mertol, W. Place, T. Webster, and R. Greif. "Detailed Loop Model (DLM) Analysis of Liquid Solar Thermosiphons with Heat Exchangers." Lawrence Berkeley Laboratory Report, LBL-10699, 1980.

16. U.S. Nuclear Regulatory Commission. Advisory Committee on Reactor Safeguards, Ad Hoc Subcommittee Meeting on Natural Circulation Heat Removal, Washington, D. C., March 26, 1980.

17. E. H. Wissler, H. S. Isbin and N. R. Amundson. "Oscillatory Behavior of a Two-Phase Natural Circulation Loop." AICHE Journal, Vol. 2, 1956, pp. 157-162.

18a. Y. Zvirin, P. R. Jeuck III, C. S. Sullivan, and R. B. Duffey. "Experimental and Analytical Investigation of a PWR Natural Circulation Loop." ANS/ENS Thermal Reactor Safety Meeting, Knoxville, Tenn., April 1980.

18b. Y. Zvirin, P. R. Jeuck III, C. S. Sullivan, and R. B. Duffey. "Experimental and Analytical Investigation of a Natural Circulation System with Parallel Loops." J. Heat Transfer, Vol. 103, 1980, (to be published).

19. M. R. Yeung, A. H. Meadows, and K. W. Turner. "Reactor Coolant System Coastdown and Natural Circulation." ANS/ENS Thermal Reactor Safety Meeting, Knoxville, Tenn., April, 1980.

20. D. J. Denver, J. F. Harrison, Jr. and N. G. Trikouros. "RETRAN Natural Circulation Analyses During the Three Mile Island Unit 2 Accident." ANS/ENS Thermal Reactor Safety Meeting, Knoxville, Tenn., April, 1980.

21. E. E. Lewis. Nuclear Power Reactor Safety. New York: Wiley, 1977.

22. J. L. Gillette, R. M. Singer, J. V. Tokar, and J. E. Sullivan. "Experimental Study of the Transition from Forced to Natural Circulation in EBR-II at Low Pressure and Flow." ASME, 79-HT-10, 1979.

23. P. W. Garrison, R. H. Morris, and B. H. Montgomery. "Natural Convection Boiling of Sodium in a Simulated FBR Fuel Assembly Subchannel." Oak Ridge National Laboratory, 1979.

24. C. V. Gregory, R. Bell, G. Brown, C. W. Dawson, J.D.C. Henderson, and R. Hampshire. "Natural Circulation Studies in Support of the Dounreay Prototype Fast Reactor (PFR)." ANS/ENS International Meeting on Fast Reactor Safety Technology, Seattle, Washington, August 1979.

25. R. P. Lowell. "Circulation in Fractures, Hot Springs and Convective Heat Transport in Mid-Ocean Ridge Crests." Geophys. J. Roy. Astron. Soc., Vol. 40, 1975, pp. 351-365.

26. K. E. Torrance. "Open-Loop Thermosyphons with Geological Applications." J. Heat Transfer, Vol. 101, 1979, pp. 677-683.

27. H. H. Bau and K. E. Torrance. "Transient and Steady Behavior of an Open, Symmetrically-Heated Free Convection Loop." Cornell Univ., Ithaca, N. Y. E80-03, 1980.

28. H. H. Bau, and E. E. Torrance. "On the Stability and Flow Reversal of an Asymmetrically-Heated Open Convection Loop." Cornell Univ., Ithaca, New York, E80-04, 1980.

29. J. B. Keller. "Periodic Oscillations in a Model of Thermal Convection." J. Fluid Mech., Vol. 26, 1966, pp. 599-606.

30. P. Welander. "On the Oscillatory Instability of a Differentially Heated Fluid Loop." J. Fluid Mech., Vol. 29, pp. 17-30.

31. H. R. McKee. "Thermosiphon Reboilers--A Review." Ind. and Eng. Chem., Vol. 62, 1970, pp. 76-82.

32. P. R. Beaver and G. A. Hughmark. "Heat Transfer Coeffcient and Circulation Rates for Thermosiphon Reboilers." AIChE Journ., Vol. 14, 1968, pp. 746-749.

33. K. C. Jain, M. Petrick, D. Miller and S. G. Bankoff. "Self-Sustained Hydrodynamic Oscillations in a Natural-Circulation Boiling Water Loop." Nuclear Eng. and Design, Vol. 4, 1966, pp. 233-252.

34. N.V.L.S. Sarma, P. J. Reddy, and P. S. Murti. "A Computer Design Method for Vertical Thermosyphon Reboilers." Ind. Eng. Chem. Process Des. Develop., Vol. 12, 1973, pp. 278-290.

35. R. T. Fernandez, J. P. Sursock, and R. L. Kiang. "Reflux Boiling Heat Removal in a Scaled TMI-2 System Test Facility." ANS/ENS Thermal Reactor Safety Meeting, Knoxville, Tenn., April, 1980.

36. H. F. Crevelng, J. F. DePaz, J. Y. Baladi and R. J. Schoenhals. "Stability Characteristics of a Single-Phase Free Convection Loop." J. Fluid Mech., Vol. 67, 1975, pp. 65-84.

37. P. S. Damerell and R. J. Schoenhals. "Flow in a Toroidal Thermosyphon with Angular Displacement of Heated and Cooled Sections." J. Heat Transfer, Vol. 101, 1979, pp. 672-676.

38. Y. Zvirin and R. Greif. "Transient Behavior of Natural Circulation Loops: Two Vertical Branches with Point Heat Source and Sink." Int. J. Heat Mass Transfer, Vol 22, 1979, pp. 499-504.

39. R. Greif, Y. Zvirin and A. Mertol. "The Transient and Stability Behavior of a Natural Circulated Loop." J. Heat Transfer, Vol. 101, 1979, pp. 684-688.

40. Y. Zvirin. "The Effect of Dissipation on Free Convection Loops." Int. J. Heat Mass Transfer, Vol. 22, 1979, pp. 1539-1546.

41. Y. Zvirin. "On the Behavior of a Natural Circulation Loop with a Through-Flow." Proc. of the 14th Intersociety Energy Conversion Engineering Conference, Boston, Massachusetts, August 1979, pp. 1974-1978.

42. Y. Zvirin. "Throughflow Effects on the Transient and Stability Characteristics of a Thermosyphon." In Advanced Energy Systems Which Maintain the Atmospheric Co_2 Balance, edited by C. W. Solbrig, Hemisphere, 1981.

43. Y. Zvirin. "The Effects of a Throughflow on the Steady State and Stability of a Natural Circulation Loop." AIChE Symposium Series, 19th National Heat Transfer Conference, Orlando, Florida, July 1980, pp. 238-249.

44. A. Mertol. "Heat Transfer and Fluid Flow in Thermosyphons." Ph.D Thesis, Dept. of Mech. Eng., University of California, Berkeley, 1980.

45. A. Mertol, R. Greif and Y. Zvirin. "The Transient, Steady-State and Stability Behavior of a Natural Convection Loop with a Throughflow." Int. J. Heat Mass Transfer, Vol. 24, 1981 (to be published).

46. J. C. Chato. "Natural Convection Flows in Parallel-Channel Systems." J. Heat Transfer, Vol. 85, 1963, pp. 339-345.

47. S. Kaizerman, E. Wacholder and E. Elias. "Numerical Simulation of a Natural Circulation Loop." Int. J. Heat Mass Transfer, Vol. 24, 1981 (to be published).

48. R. L. Kiang, P. R. Jeuck and J. S. Marks. SRI Int. private communication, 1980.

49. A. Bartal-Bornstein. "Research into the Stability of Thermosyphonic Flows in System Utilizing Solar Energy." M.S. thesis, faculty of Mech. Eng. Technion, Haifa, Israel [in Hebrew], Oct. 1977.

50. U.S. Nuclear Regulatory Commission. "Generic Evaluation of Feedwater Transients and Small Break Loss-of-Coolant Accidents in Westinghouse-Designed Operating Plants." Ch. VII--Natural Circulation. NUREG-0611, Jan. 1980.

51. U.S. Nuclear Regulatory Commission. "Generic Evaluation of Transients and Small Break Loss-of-Coolant Accidents in Combustion Engineering." Designed Operating Plants, Ch. VII--Natural Circulation. NUREG-0635, Jan. 1980.

52. U.S. Nuclear Regulatory Commission. "Generic Evaluation of Small Break Loss-of-Coolant Accident Behavior in Babcock & Wilcox Designed 177-FA Operating Plant. NUREG-0565, Jan. 1980.

APPENDIX A

SUMMARY OF NATURAL CIRCULATION PLANT DATA

	PLANT	TYPE/ POWER MW	DATE	TEST/INCIDENT	STEADY OR QUASI STEADY STATE CORE POWER MW	ΔT MEAS. °C	ΔT CAL. °C	$\dot{M}$ Kg/s	REMARKS
1	OCONEE 1	B&W 860	5/1/73	N.C.- IMPOSED BY PRESSURE DECREASE IN SG - NO INPUT POWER	0				TRANSIENT (30 MIN.) TOWARDS NEW SS AT THE LOWER TEMP.
2	OCONEE-1	"	11/4/73	TEST-LOSS OF OFFSITE POWER	27	17	20	378	TRANSIENT OF 22 MIN., QUASI STUDY STATE
3	OCONEE-1	"	5/2/74	TEST - NATURAL CIRCULATION	49	14	30	833	TRANSIENT OF 37 MIN., QUASI STEADY STATE TEMPS, SG LEVEL CHANGING
4	OCONEE-2	"	1/4/74	REACTOR TRIP FOLLOWING SEPARATION FROM GRID	20	28	16	170	LONG TRANSIENT, DATA UNTIL 100 MIN-QUASI STEADY STATE. HPIS KEPT CONSTANT
5	ANO -1	B&W 836	2/22/75	LOSS OF ELECTRICAL POWER	65	16	36	967	TRANSIENT OF ONLY 5 MIN. FAR FROM STEADY STATE
6	CRYSTAL RIVER 3	B&W 858	4/23/77	TEST-LOSS OF OFFSITE POWER	12	24	12	122	TRANSIENT OF 20 MIN NON-SYMMETRICAL LOOPS OPERATION, QUASI STEADY STATE NOT FULLY ESTAB-LISHED, SG LEVEL CHANGING

SUMMARY OF NATURAL CIRCULATION PLANT DATA

STEADY OR QUASI STEADY STATE

	PLANT	TYPE/ POWER MW	DATE	TEST/INCIDENT	CORE POWER MW	ΔT MEAS. °C	ΔT CAL. °C	$\dot{M}$ Kg/s	REMARKS
7	TMI -2	B&W 880	4/22/78	TEST-LOSS OF OFFSITE POWER	10	19	10	131	TRANSIENT OF 40 MIN. OSCILLATIONS IN TEMP-ERATURES, STRONG IN COLD LEG B
8	DAVIS BESSE 1	B&W 906	12/3/78	TEST-LOSS OF OFFSITE POWER	22	17	18	308	TRANSIENT OF 14 MIN. QUASI STEADY STATE NOT REACHED, SECONDARY PRESSURE CHANGING
9	DAVIS BESSE 1	"	1/15/79	TEST-LOSS OF OFFSITE POWER	16	15	14	254	TRANSIENT OF 9 MIN., APPARENT QUASI-STEADY STATE
10	DAVIS BESSE 1	"	12/3/78	TEST-NATURAL CIRCULATION	107	22	50	1160	CONSTANT POWER, STEADY STATE TEMPS, OSCILLATIONS IN SG LEVELS
11	KEWAUNEE	W 2 ? 535	4/26/75 5:30 P.M.	BACKDOWN AND SHUTDOWN DUE TO HOT RESERVE AUX.BUS. RC PUMPS TRIPPED: 9P.M.(B) AND 7:15AM 4/27 (A)		13			NATURAL CIRCULATION TRANSIENT OF 2 DAYS UNTIL RHR ON. STEADY STATE
12	KEWAUNEE	"	1/17/77 0:45AM	SHUTDOWN DUE TO TURBINE BLADE BURST. SWITCH TO NATURAL CIRCULATION TO REDUCE LOAD 2:20AM		6			NATURAL CIRCULATION TRANSIENT OF 2 DAYS UNTIL RHR ON . STEADY STATE

SUMMARY OF NATURAL CIRCULATION PLANT DATA

	PLANT	TYPE/ POWER MW	DATE	TEST/INCIDENT	STEADY OR QUASI STEADY STATE CORE POWER MW	ΔT MEAS. °C	$\overline{\Delta T}$ CAL. °C	$\dot{M}$ kg/s	REMARKS
13	KEWAUNEE	W 2ℓ 535	1/17/80	LOSS OF OFFSITE POWER		~10			TRANSIENT OF 9 HOURS UNTIL RHR ON. QUASI STEADY STATE
14	PALISADES	CE 798	4/20/72	TEST-NATURAL CIRCULATION	11.4	8		339	TRANSIENT OF 45 MIN. NEARLY QUASI STEADY STATE
15	YANKEE ROWE	W 4ℓ 175		TEST-LOSS OF OFFSITE POWER	3.9	9		103	TRANSIENT OF 3 HOURS STEADY STATE
16	PRAIRIE ISLAND	W 2ℓ 520	10/2/79	TUBE BREAK IN SG PUMPS STOPPED AFTER 13 MIN.	SOFTWARE DATA FOR 200 SCATTERED	DATA	SEC. AND SOME		TRANSIENT OF 16 HOURS UNTIL RHR ON. INJECTION OF WATER TO MAKE UP FOR LEAKS.
17	TROJAN	W 4ℓ 1130	2/14/76	TEST-NATURAL CIRCULATION	136	25	34	1290	TRANSIENT OF 100 MIN (FROM START UP) STEADY STATE RETRAN CALCULATIONS FAIR AGREEMENT WITH TRANSIENT DATA
18	TMI -2	B&W 880	3/28/79 4/27/79	ACCIDENT SWITCH TO NATURAL CIRCULATION	2.5	8	9		CALCULATIONS BASED ON ESTIMATED CORE BLOCKAGE (K_{CORE}= 60K NOMINAL) RETRAN CALCULATIONS FAIR AGREEMENTS. ALSO CADDS/ NATURAL B&W
19	SEQUOYAH	W 4ℓ 1148	6/79	TEST - NATURAL CIRCULATION					PRE-TEST RETRAN CALCULATIONS
20	NORTH ANA -2	W 3ℓ 939	7/80	TEST - NATURAL CIRCULATION	84 (3%)	20-22	12		CALCULATION BASED ON ASSUMED LOOP FLOW RESISTANCE

SUMMARY OF NATURAL CIRCULATION PLANT DATA

	PLANT	TYPE/ POWER MW	DATE	TEST/INCIDENT	STEADY OR QUASI STEADY STATE CORE POWER MW	ΔT MEAS. °C	ΔT CAL. °C	$\dot{M}$ Kg/s	REMARKS
21	POINT BEACH (ref.[50])	W 2ℓ 497		TEST - NATURAL CIRCULATION	39.6	A B 7 9 11 12		A % B 13.7 5.8 15.3 9.5	
22	HADDAM NECK (ref.[50])	W 4ℓ 527		TEST - NATURAL CIRCULATION				3.2%	TEST INITIATED BY PUMPS TRIP 1 HOUR AFTER REACTOR SHUTDOWN, FOLLOWING A MONTH OF OPERATION AT 70% POWER
23	ZION - 1 (REF. 50)	W 4ℓ 1040		TEST- NATURAL CIRCULATION	32.5 (1%) 130 (4%)			3,28% 52%	SEE RESULTS IN FIG. 14
24	FT. CALHOUN (ref.[51])	CE 457		TEST- NATURAL CIRCULATION	7.1 (0.5%)				TYPICAL RESULTS IN FIG.15
25	CALVERT CLIFFS (ref.[51])	CE 845		TEST- NATURAL CIRCULATION	14(0.53%)				TYPICAL RESULTS IN FIG. 15
26	ST. LUCIE 1 (ref.[51])	CE 810		TEST- NATURAL CIRCULATION	14.2(0.56%)				TYPICAL RESULTS IN FIG. 15
27	ST. LUCIE	CE 810	6/11/80	LOSS OF OFF SITE POWER	3% ASSUMED	14	12		$\Delta T=14^{\circ}$ FROM ~1HR AFTER REACTOR SCRAM. PRESSURIZER LEVEL CONTROLLED BY SPRAYING, TO FILL VOID IN THE REACTOR DOME CAUSED BY DEPRESSURIZATION. SEE FIG. 16
28	ST. LUCIE	CE 810	4/15/80	LOSS OF OFF SITE POWER					BEHAVIOR SIMILAR TO INCIDENT ON 6/11/80. THE DEPRESSURIZATION AND PRESSURIZATION CONTROL WERE SLOWER. SEE FIG. 16

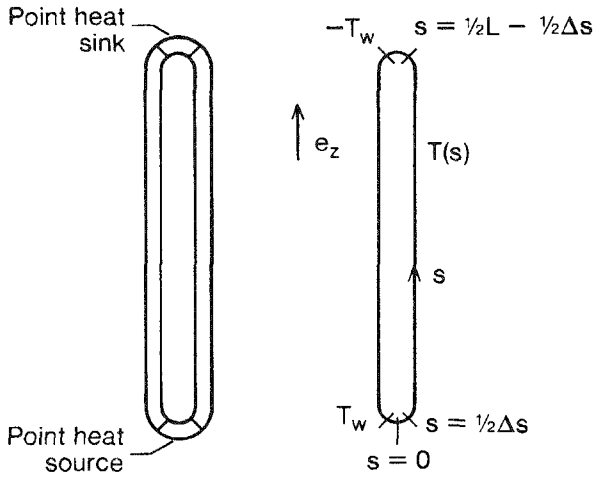

(a) Vertical loop [29, 30, 38, 40–43]

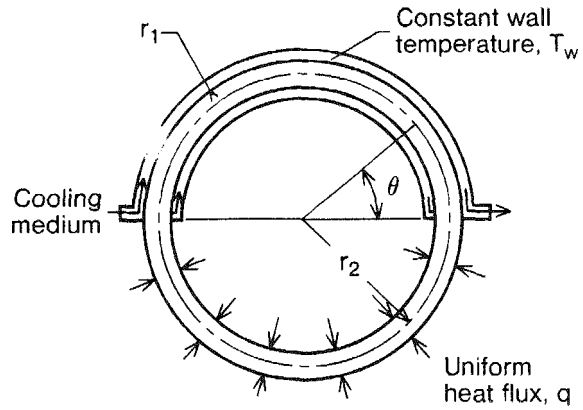

(b) Toroidal loop [36, 37, 39, 40, 44, 45]

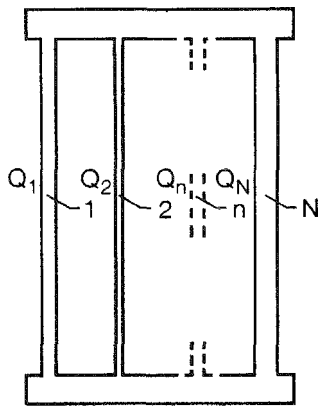

(c) Parallel branches [46]

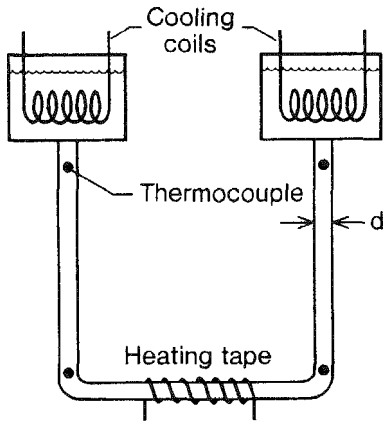

(d) Open "square" loop [26–28]

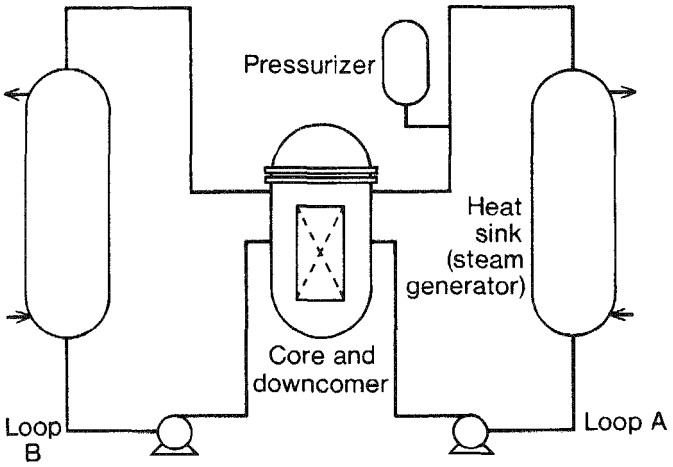

(e) Parallel heat sinks loop relevant to PWR's [18–21, 35, 50, 51]

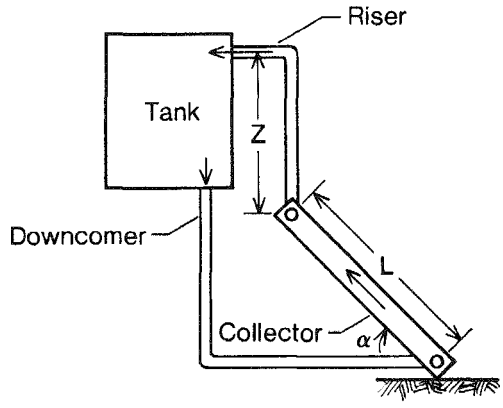

(f) Solar heater [6–10, 12–15]

Figure 1.

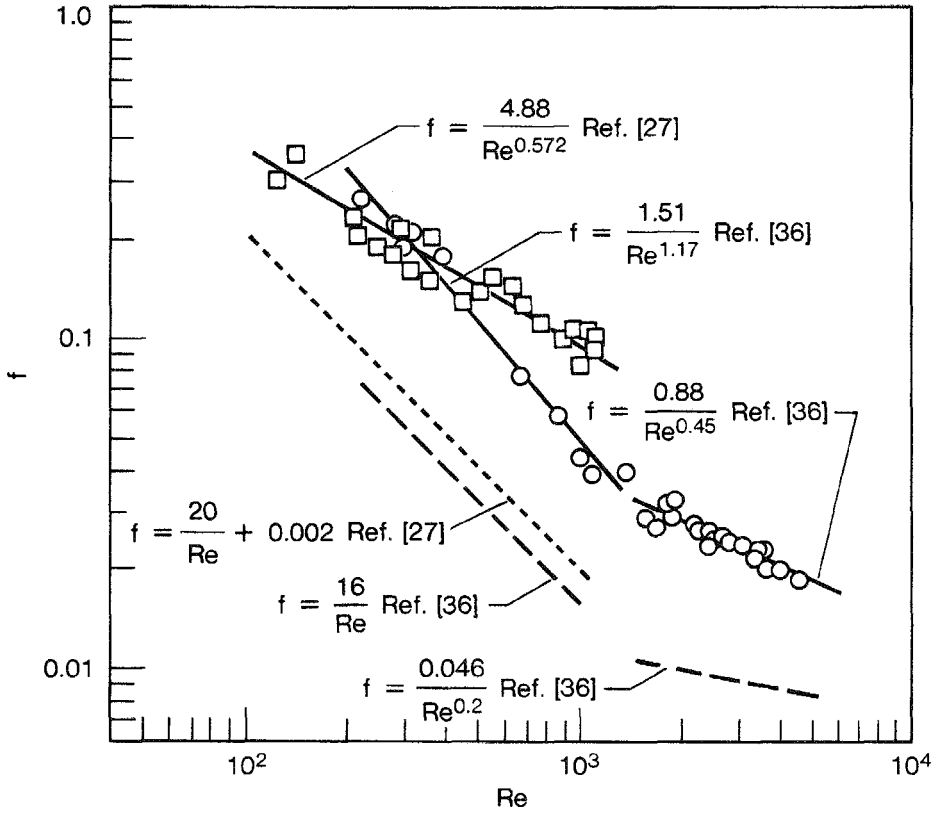
1.0
0.1
0.01
f
$f = \frac{4.88}{Re^{0.572}}$ Ref. [27]
$f = \frac{1.51}{Re^{1.17}}$ Ref. [36]
$f = \frac{0.88}{Re^{0.45}}$ Ref. [36]
$f = \frac{20}{Re} + 0.002$ Ref. [27]
$f = \frac{16}{Re}$ Ref. [36]
$f = \frac{0.046}{Re^{0.2}}$ Ref. [36]
10^2
10^3
10^4
Re

Figure 2.

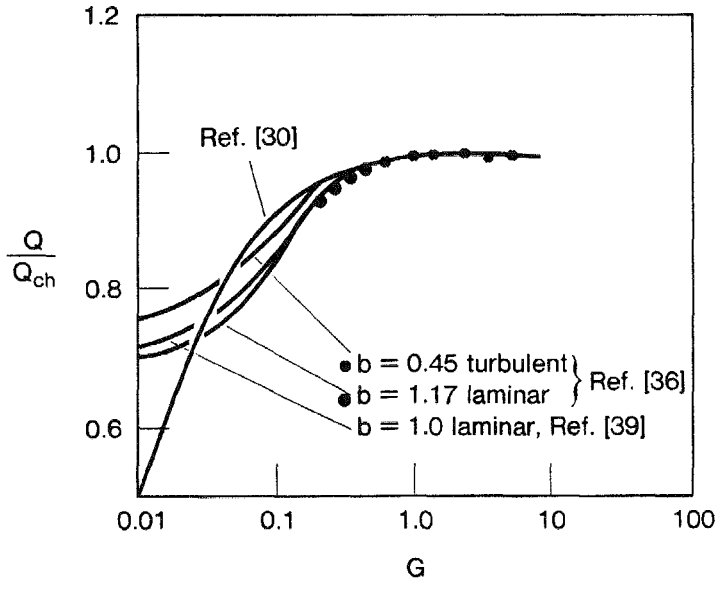

Figure 3a.

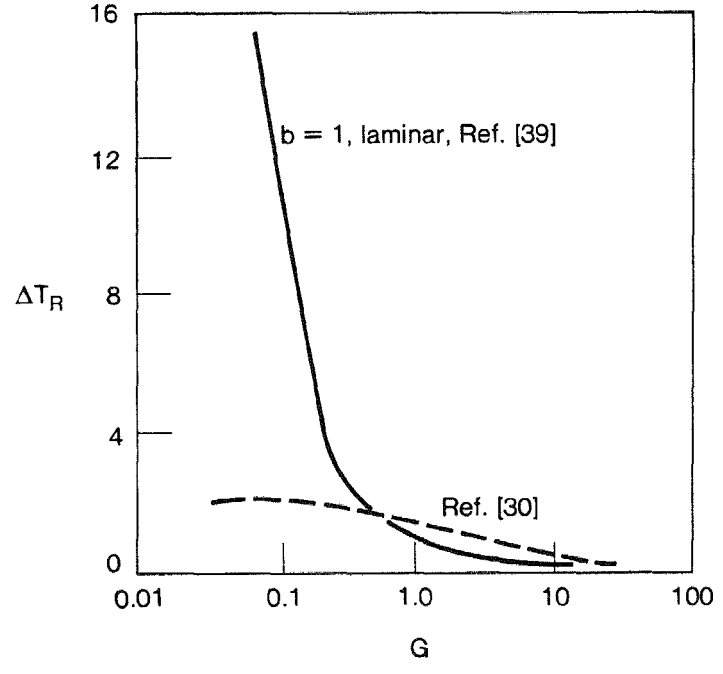

Figure 3b.

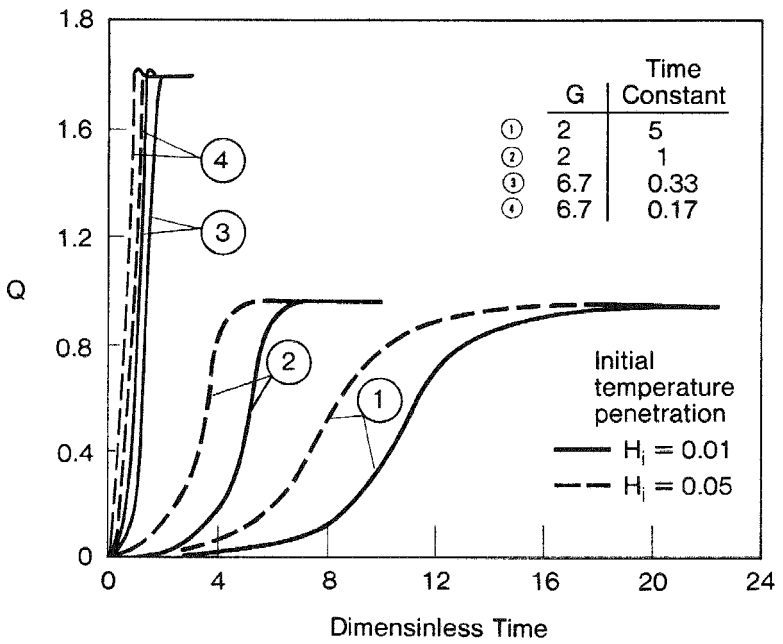
1.8
1.6
1.2
0.8
0.4
0
Q
0
4
8
12
16
20
24
Dimensinless Time
Time
G
Constant
① 2 5
② 2 1
③ 6.7 0.33
④ 6.7 0.17
Initial
temperature
penetration
$H_i = 0.01$
$H_i = 0.05$
1
2
3
4

Figure 4.

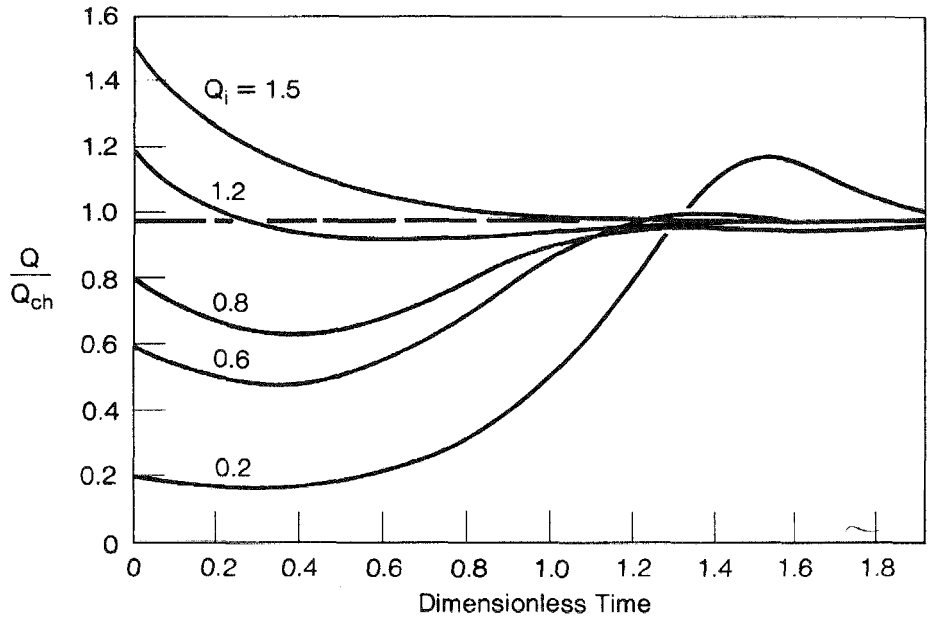

Figure 5a.

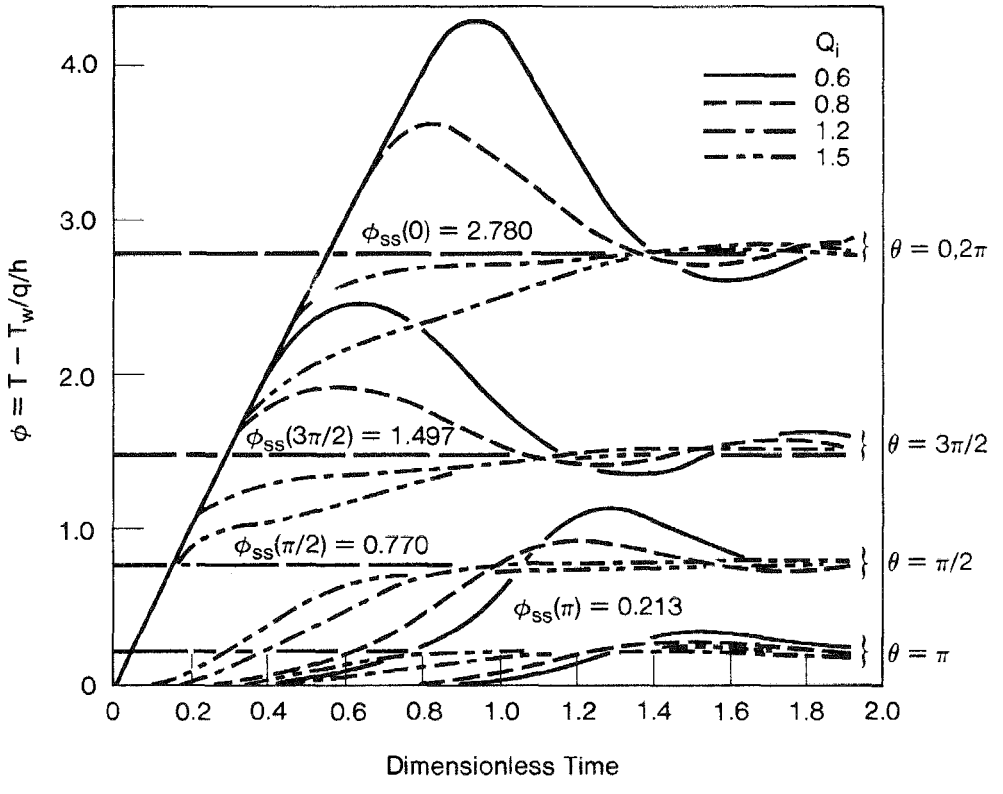

Figure 5b.

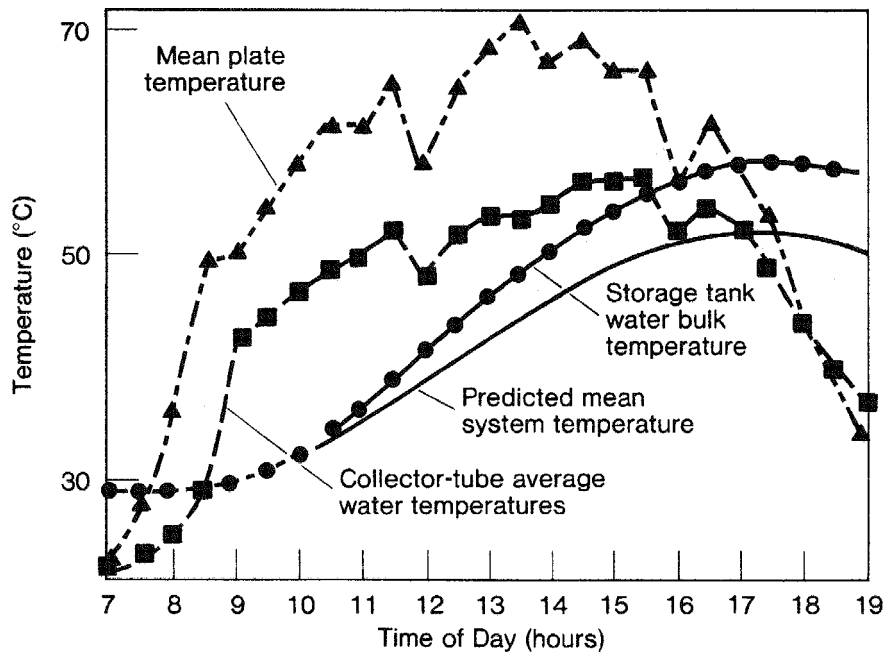
70
50
30
Temperature (°C)
Mean plate temperature
Storage tank water bulk temperature
Predicted mean system temperature
Collector-tube average water temperatures
7
8
9
10
11
12
13
14
15
16
17
18
19
Time of Day (hours)

Figure 6.

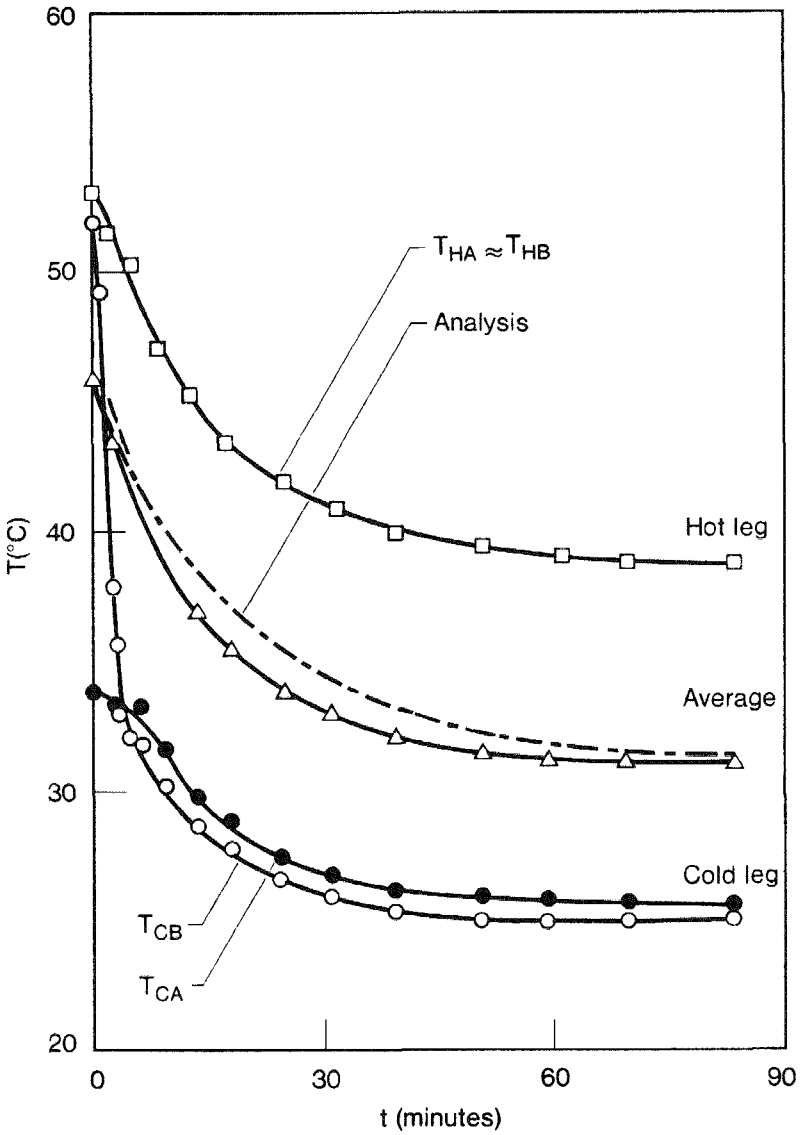
60
50
40
30
20
T(°C)
0
30
60
90
t (minutes)
$T_{HA} \approx T_{HB}$
Analysis
Hot leg
Average
Cold leg
T_{CB}
T_{CA}

Figure 7.

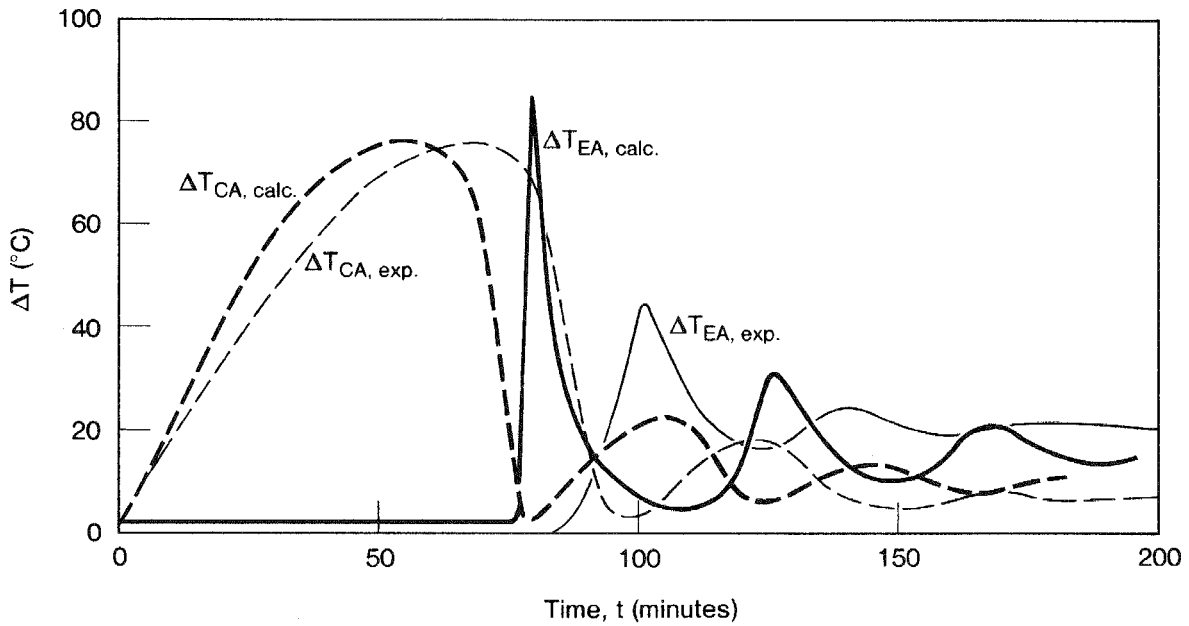
100
80
60
40
20
0
ΔT (°C)
0
50
100
150
200
Time, t (minutes)
ΔT CA, calc.
ΔT CA, exp.
ΔT EA, calc.
ΔT EA, exp.

Figure 8a.

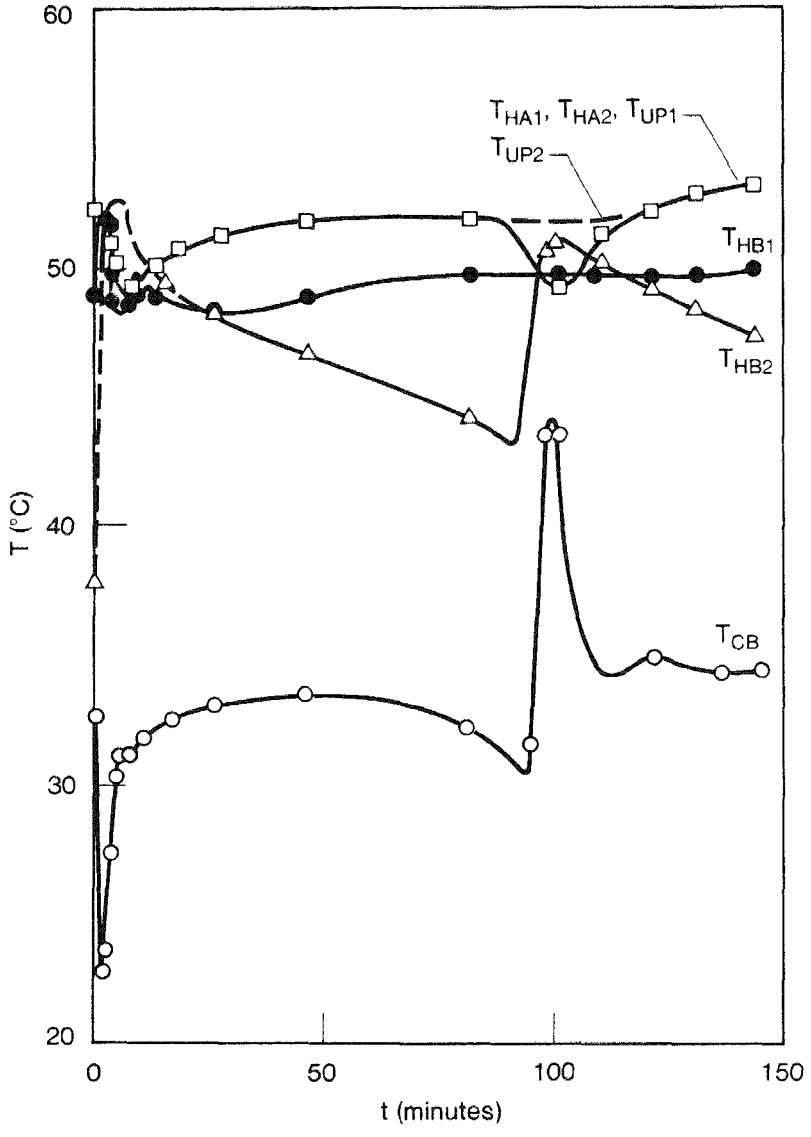
60
50
40
30
20
T (°C)
0
50
100
150
t (minutes)
T_{HA1}, T_{HA2}, T_{UP1}
T_{UP2}
T_{HB1}
T_{HB2}
T_{CB}

Figure 8b.

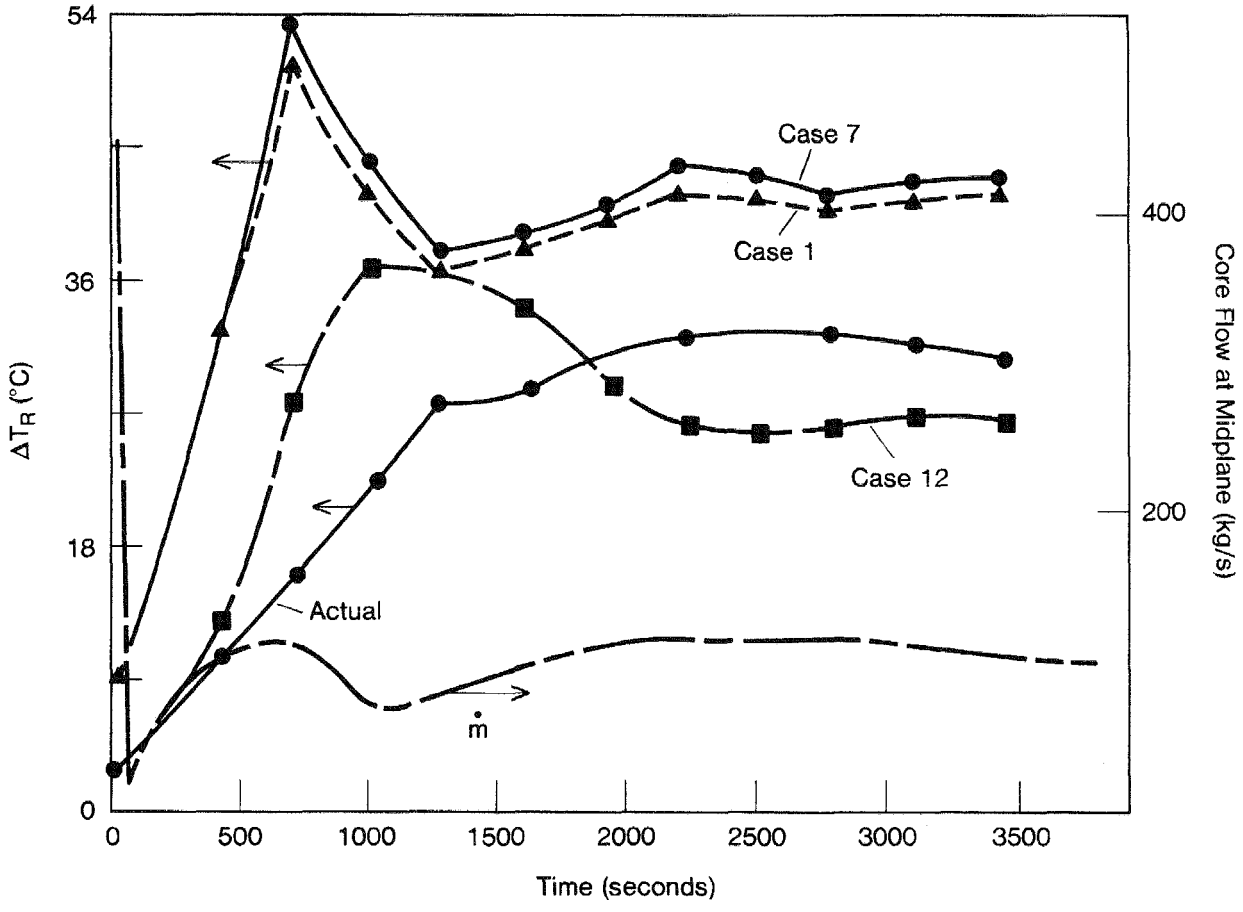
54
36
18
0
ΔT_R (°C)
0
500
1000
1500
2000
2500
3000
3500
Time (seconds)
Case 7
Case 1
Case 12
Actual
$\dot{m}$
400
200
Core Flow at Midplane (kg/s)

Figure 9.

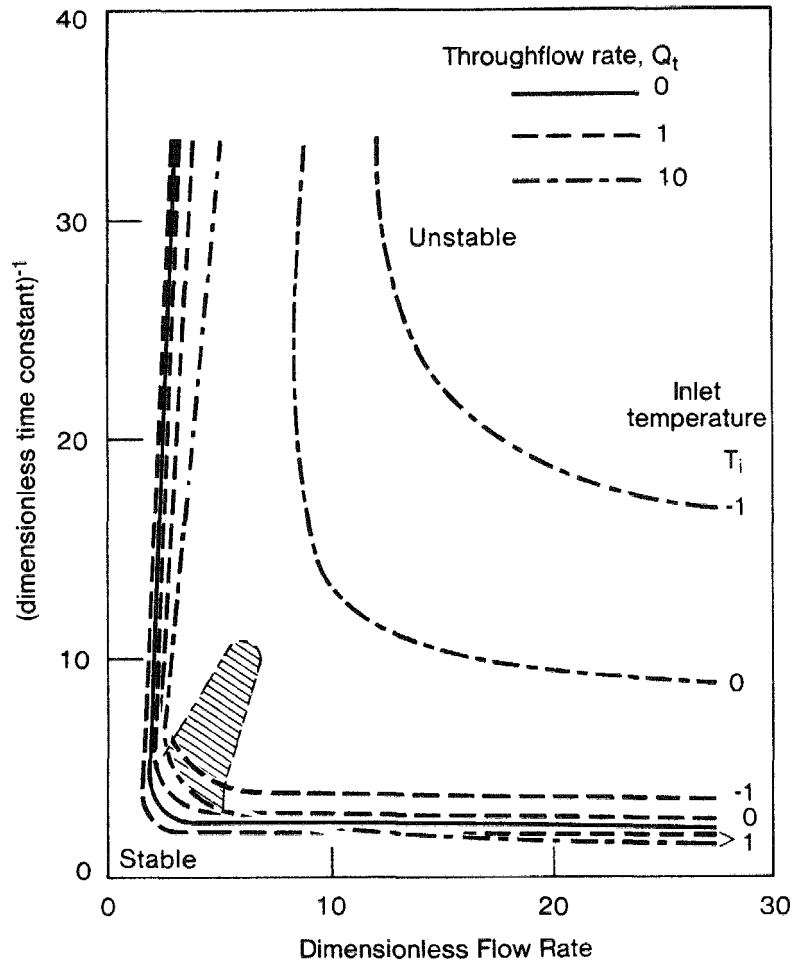
Throughflow rate, Q_t
0
1
10
Unstable
Inlet temperature T_i
-1
0
-1
0
1
Stable
40
30
20
10
0
0
10
20
30
(dimensionless time constant)$^{-1}$
Dimensionless Flow Rate

Figure 10a.

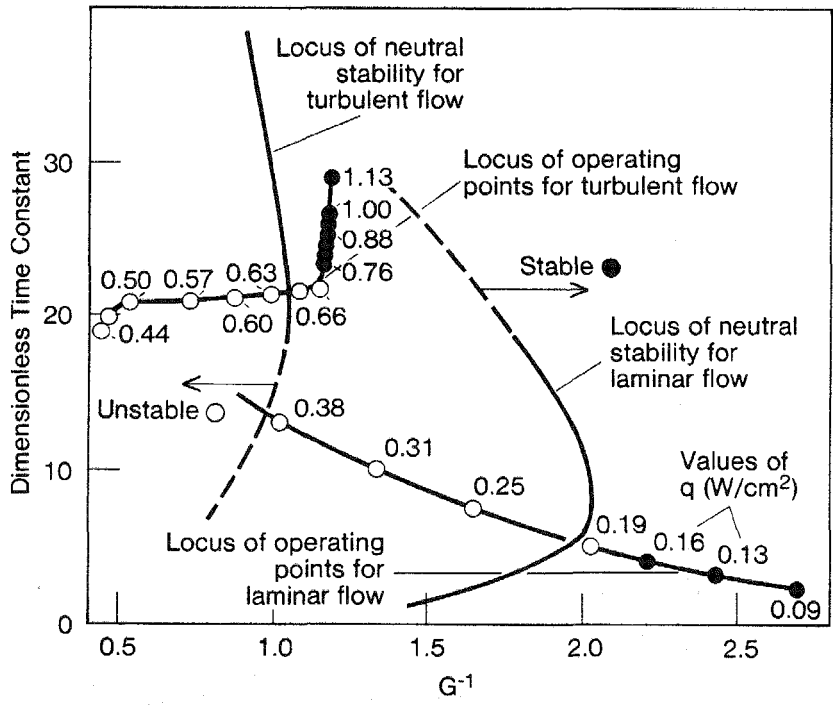
Locus of neutral stability for turbulent flow
Locus of operating points for turbulent flow
1.13
1.00
0.88
0.76
Stable
0.50
0.57
0.63
0.60
0.66
0.44
Locus of neutral stability for laminar flow
Unstable
0.38
0.31
0.25
Values of q (W/cm²)
0.19
0.16
0.13
0.09
Locus of operating points for laminar flow
Dimensionless Time Constant
30
20
10
0
0.5
1.0
1.5
2.0
2.5
G⁻¹

Figure 10b.

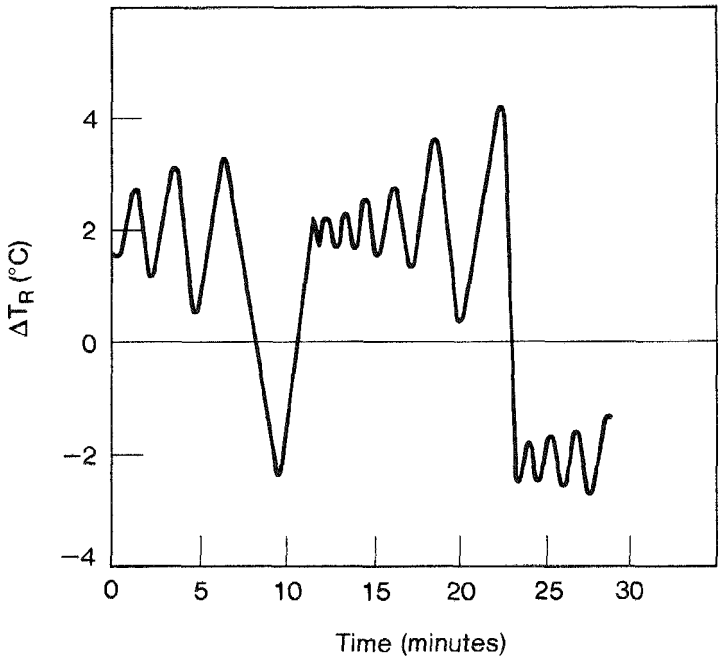

Figure 10c.

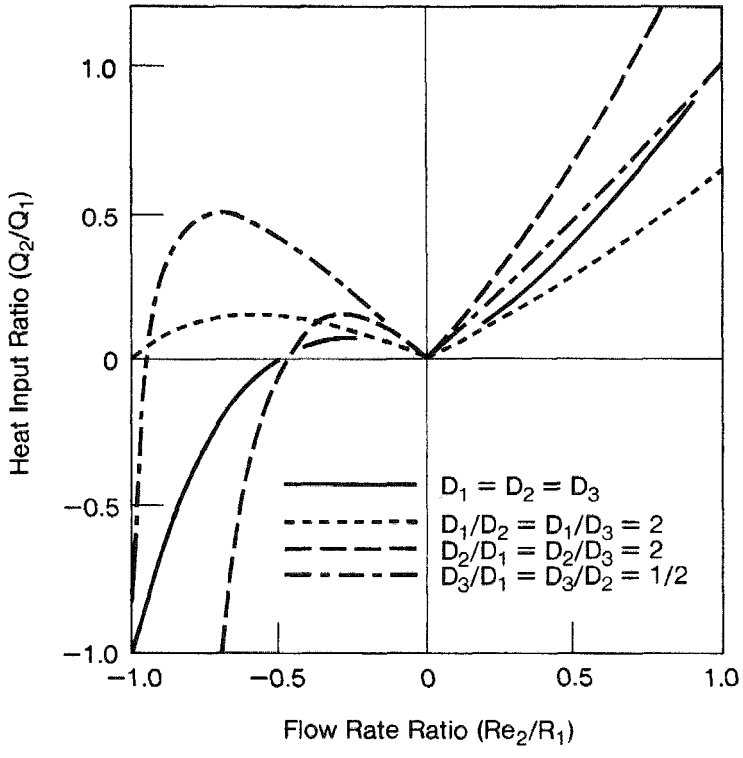
1.0
0.5
0
−0.5
−1.0
−1.0
−0.5
0
0.5
1.0
Heat Input Ratio (Q_2/Q_1)
Flow Rate Ratio (Re_2/R_1)
$D_1 = D_2 = D_3$
$D_1/D_2 = D_1/D_3 = 2$
$D_2/D_1 = D_2/D_3 = 2$
$D_3/D_1 = D_3/D_2 = 1/2$

Figure 11a.

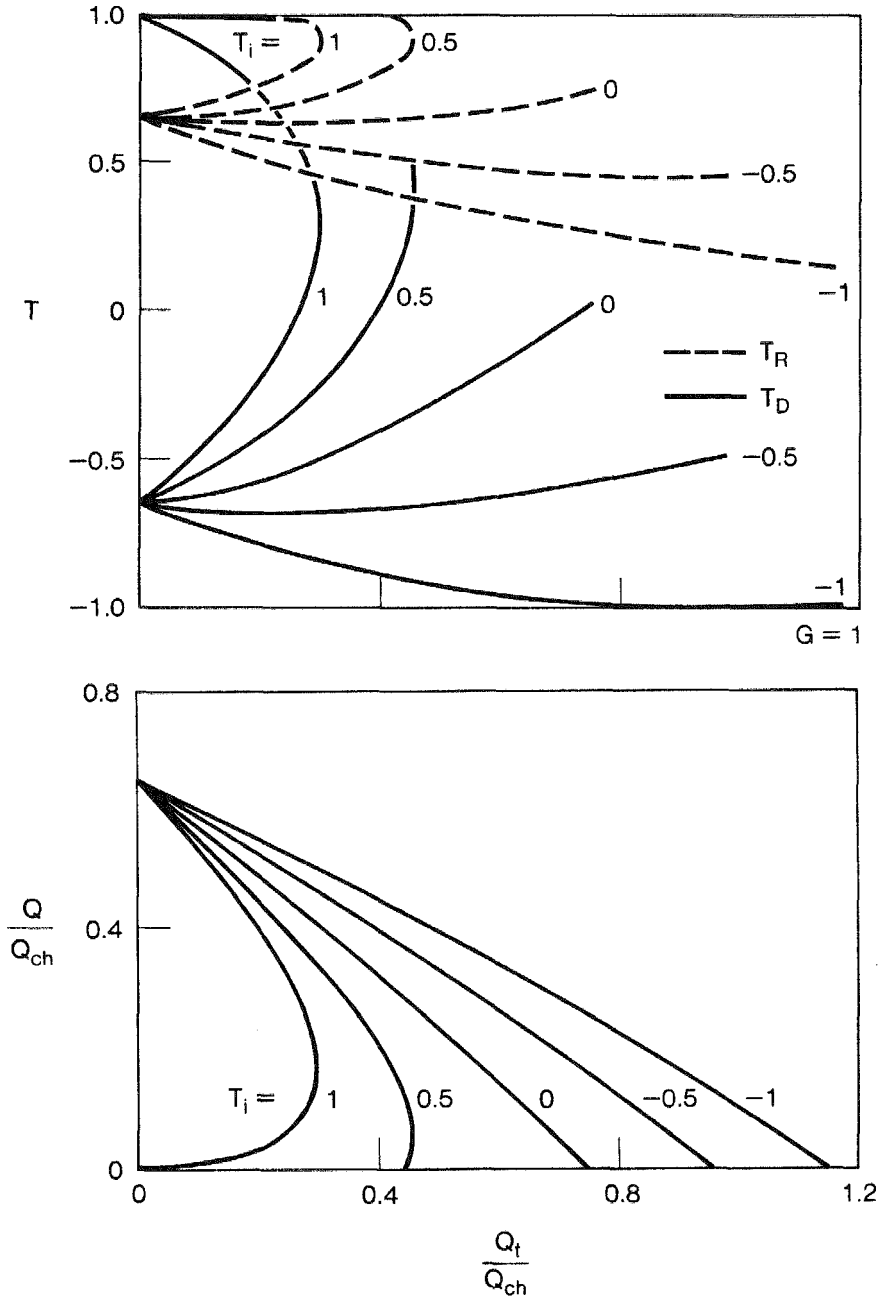

Figure 11b.

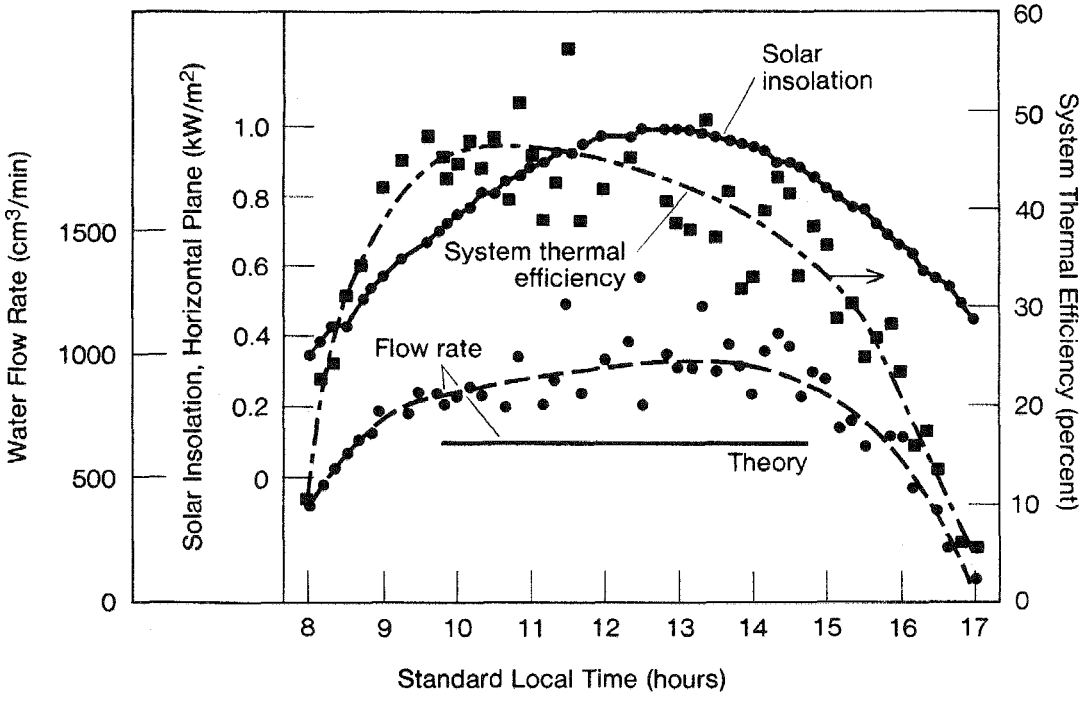
Water Flow Rate (cm³/min)
Solar Insolation, Horizontal Plane (kW/m²)
System Thermal Efficiency (percent)
Standard Local Time (hours)
Solar insolation
System thermal efficiency
Flow rate
Theory
0
500
1000
1500
0
0.2
0.4
0.6
0.8
1.0
0
10
20
30
40
50
60
8
9
10
11
12
13
14
15
16
17

Figure 12a.

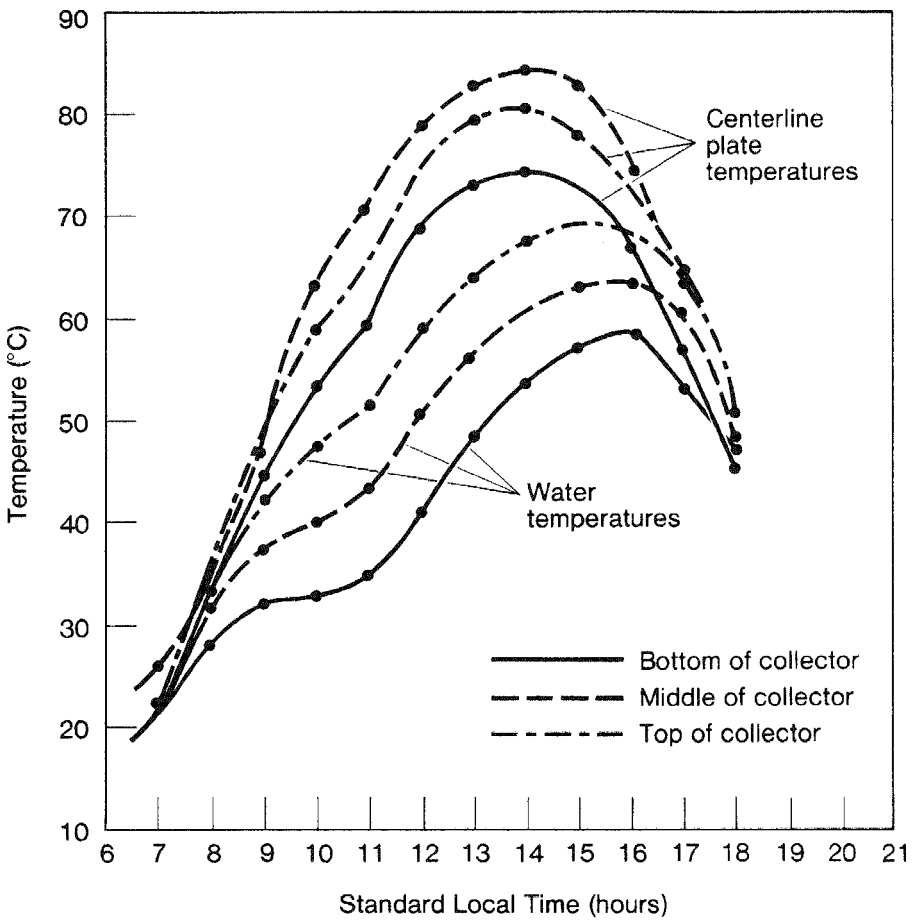
90
80
70
60
50
40
30
20
10
Temperature (°C)
6
7
8
9
10
11
12
13
14
15
16
17
18
19
20
21
Standard Local Time (hours)
Centerline plate temperatures
Water temperatures
Bottom of collector
Middle of collector
Top of collector

Figure 12b.

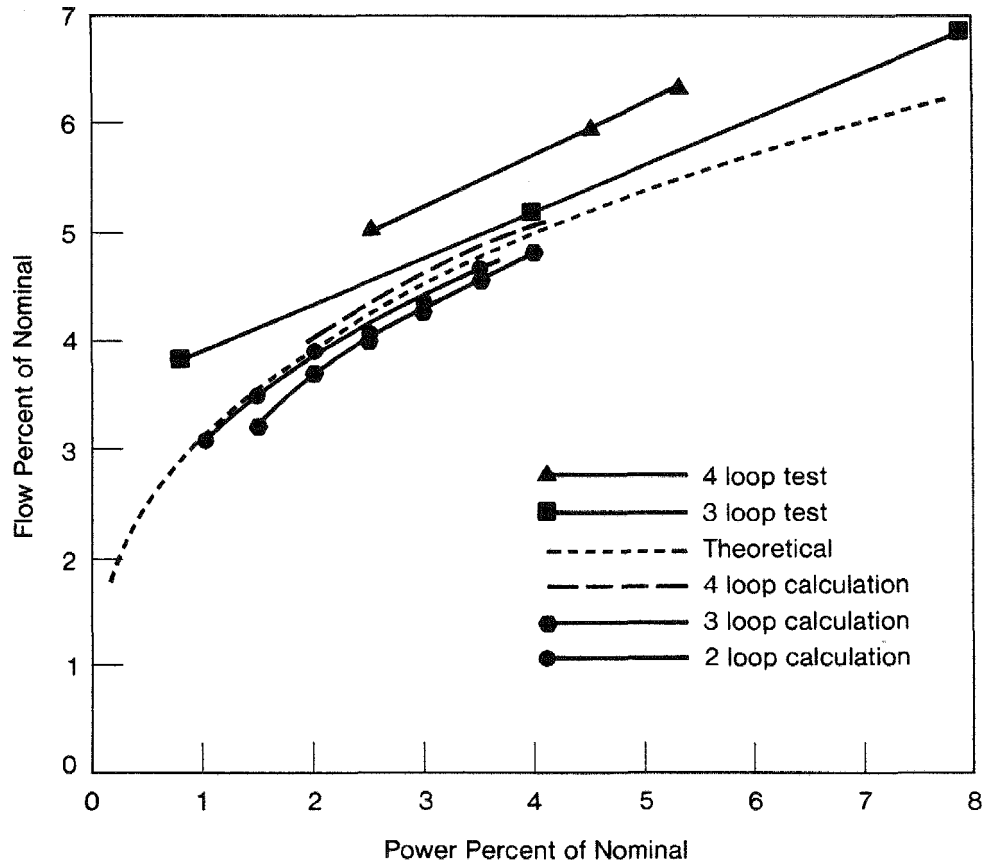
Flow Percent of Nominal
Power Percent of Nominal
0
1
2
3
4
5
6
7
8
4 loop test
3 loop test
Theoretical
4 loop calculation
3 loop calculation
2 loop calculation

Figure 13.

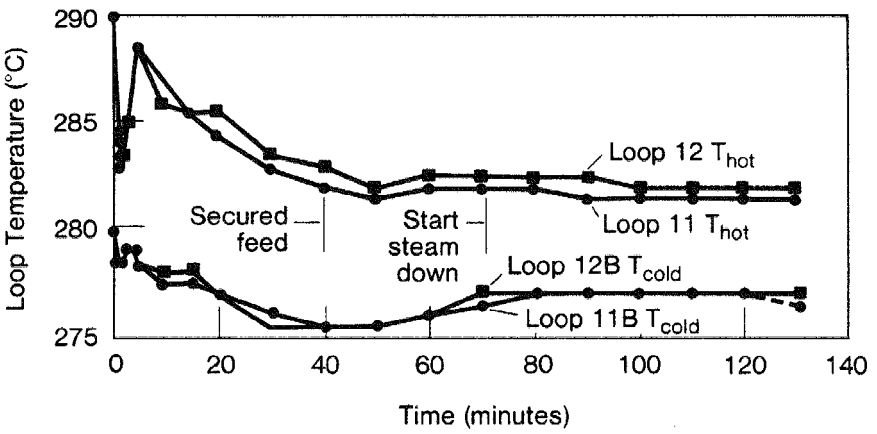
290
285
280
275
Loop Temperature (°C)
Secured feed
Start steam down
Loop 12 T_{hot}
Loop 11 T_{hot}
Loop 12B T_{cold}
Loop 11B T_{cold}
0
20
40
60
80
100
120
140
Time (minutes)

Figure 14.

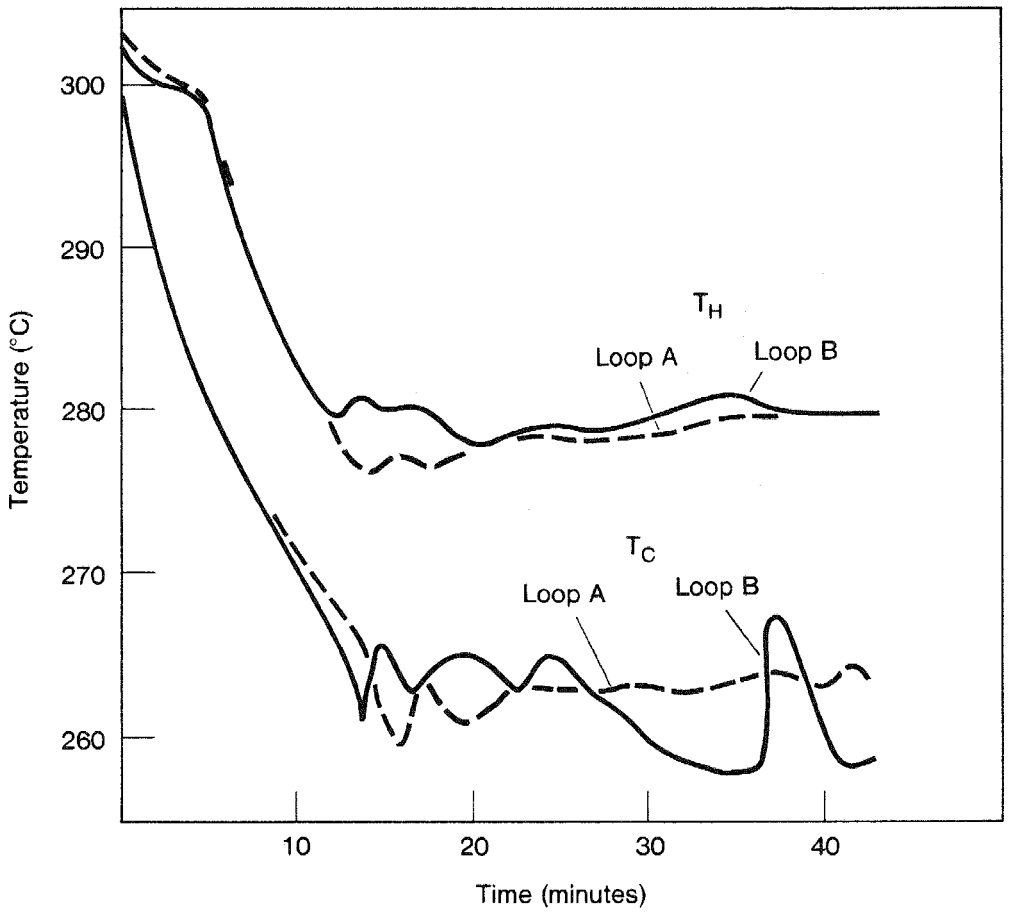
300
290
280
270
260
Temperature (°C)
T_H
Loop A
Loop B
T_C
Loop A
Loop B
10
20
30
40
Time (minutes)

Figure 15a.

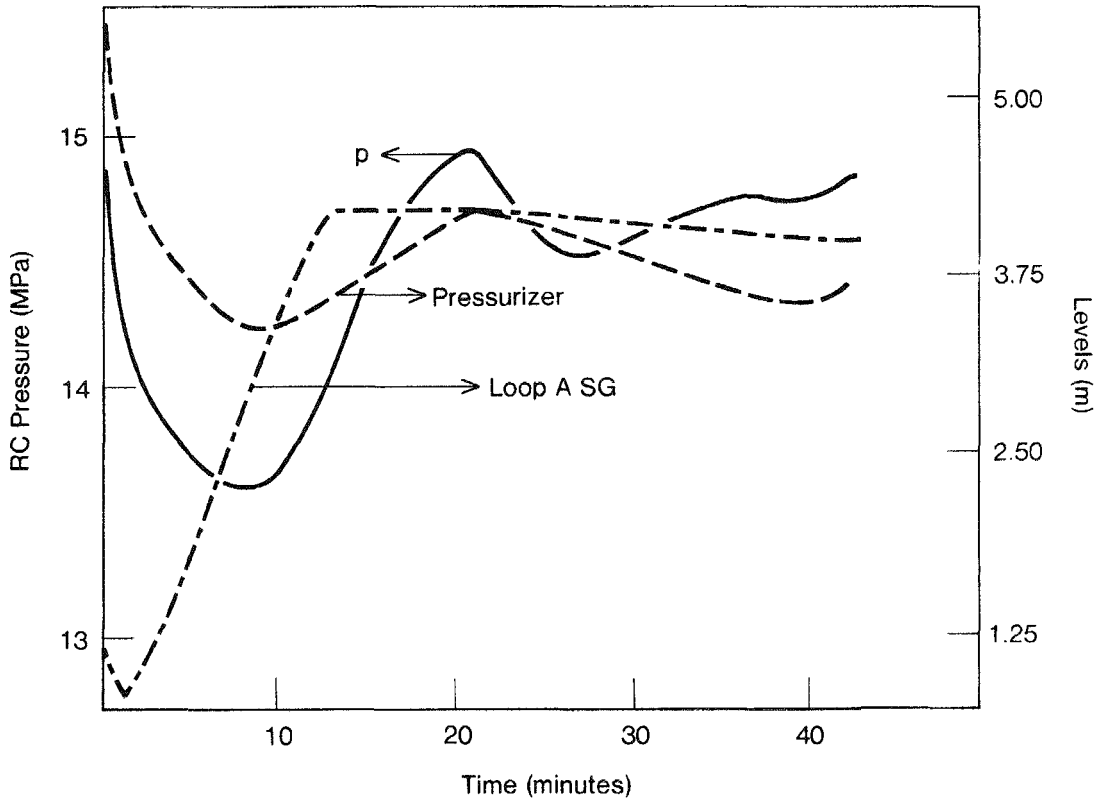
RC Pressure (MPa)
15
14
13
p
Pressurizer
Loop A SG
5.00
3.75
2.50
1.25
Levels (m)
10
20
30
40
Time (minutes)

Figure 15b.

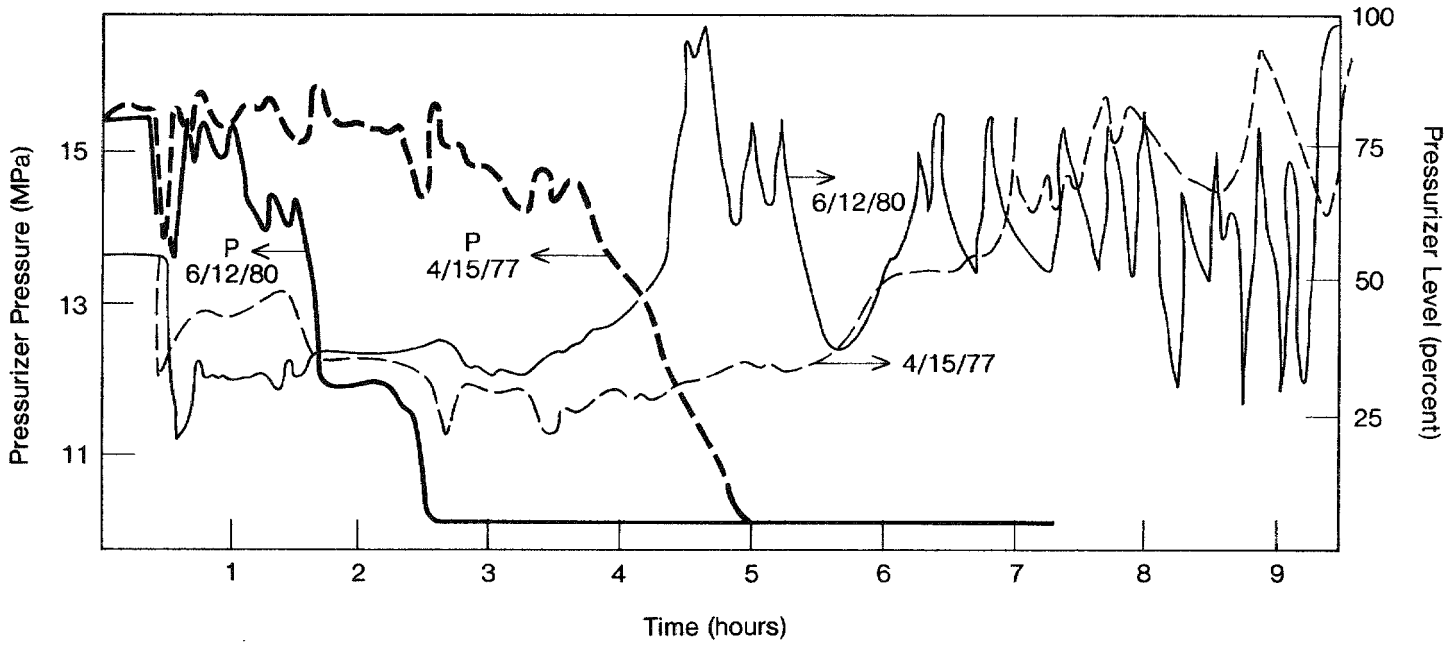
Pressurizer Pressure (MPa)
15
13
11
P
6/12/80
P
4/15/77
6/12/80
4/15/77
100
75
50
25
Pressurizer Level (percent)
1
2
3
4
5
6
7
8
9
Time (hours)

Figure 16.